DAFTAR PUSTAKA

Abualnaja, K. M., Alprol, A. E., Abu-Saied, M. A., Mansour, A. T., & Ashour, M. (2021). Studying the adsorptive behavior of poly(Acrylonitrile-co-styrene) and carbon nanotubes (nanocomposites) impregnated with adsorbent materials towards methyl orange dye. *Nanomaterials*, *11*(5), 1–22.

Ajaz, M., Shakeel, S., & Rehman, A. (2020). Microbial use for azo dye degradation—a strategy for dye bioremediation. *International Microbiology*, *23*(2), 149–159.

Akbal, F. (2005). Sorption of phenol and 4-chlorophenol onto pumice treated with cationic surfactant. *Journal of Environmental Management*, *74*(3), 239–244.

Alabi, F. M., Lajide, L., Ajayi, O. O., Adebayo, A. O., Emmanuel, S., & Fadeyi, A. E. (2020). Synthesis and characterization of carboxymethyl cellulose from Musa paradisiaca and Tithonia diversifolia. *African Journal of Pure and Applied Chemistry*, *14*(1), 9–23.

Albukhari, S. M., Ismail, M., Akhtar, K., & Danish, E. Y. (2019). Catalytic reduction of nitrophenols and dyes using silver nanoparticles @ cellulose polymer paper for the resolution of waste water treatment challenges. *Colloids and Surfaces A: Physicochemical and Engineering Aspects*, *577*, 548–561.

Alghamdi, A. A., Al-Odayni, A. B., Saeed, W. S., Almutairi, M. S., Alharthi, F. A., Aouak, T., & Al-Kahtani, A. (2019). Adsorption of azo dye methyl orange from aqueous solutions using alkali-activated polypyrrole-based graphene oxide. *Molecules*, *24*(20), 2–17.

Alhujaily, A., Yu, H., Zhang, X., & Ma, F. (2018). Highly efficient and sustainable spent mushroom waste adsorbent based on surfactant modification for the removal of toxic dyes. *International Journal of Environmental Research and Public Health*, *15*(7), 1–15.

Ali, S. M., & Eskandrani, A. A. (2020). The sorption performance of Cetyl Trimethyl Ammonium Bromide-Capped La0.9Sr0.1FeO3 perovskite for organic pollutants from industrial processes. *Molecules*, *25*(7), 1–15.

Anita, S. H., Sari, F. P., & Yanto, D. H. Y. (2019). Decolorization of synthetic dyes by ligninolytic enzymes from trametes hirsuta D7. *Makara Journal of Science*, *23*(1), 44–50.

Asem, M., Jimat, D. N., Jafri, N. H. S., Wan Nawawi, W. M. F., Azmin, N. F. M., & Abd Wahab, M. F. (2021). Entangled cellulose nanofibers produced from sugarcane bagasse via alkaline treatment, mild acid hydrolysis assisted with ultrasonication. *Journal of King Saud*

University - Engineering Sciences, 1–8.

Ashna, P., & Heydari, R. (2020). Removal of reactive red 198 from aqueous solutions using modified clay: optimization, kinetic and isotherm. *Journal of the Chilean Chemical Society*, *4*, 4958–4961.

Atkins, P. W. (1997). *Kimia fisika edisi keempat jilid 2*. Jakarta: Erlangga.

Baena-Baldiris, D., Montes-Robledo, A., & Baldiris-Avila, R. (2020). Franconibacter sp ., 1MS: A new strain in decolorization and degradation of azo dyes ponceau s red and methyl orange. *ACS Omega*, *5*(43), 28146–28157.

Baetens, R., Jelle, B. P., & Gustavsen, A. (2011). Aerogel insulation for building applications: A state-of-the-art review. *Energy and Buildings*, *43*(4), 761–769.

Bahrudin, N. N., & Nawi, M. A. (2019). Mechanistic of photocatalytic decolorization and mineralization of methyl orange dye by immobilized TiO2/chitosan-montmorillonite. *Journal of Water Process Engineering*, *31*, 1–14.

Bamroongwongdee, C., Gaewkhem, S., & Siritrakul, P. (2018). Kinetics, Equilibrium, and Thermodynamics of Methyl Orange Adsorption onto Modified Rice Husk. *KMUTNB International Journal of Applied Science and Technology*, *11*(3), 185–197. https://doi.org/10.14416/j.ijast.2018.05.002

Bamroongwongdee, C., Suwannee, S., & Kongsomsaksiri, M. (2019). Adsorption of congo red from aqueous solution by surfactant-modified rice husk: Kinetic, isotherm and thermodynamic analysis. *Songklanakarin Journal of Science and Technology*, *41*(5), 1076–1083.

Banjare, M. K., Kurrey, R., Yadav, T., Sinha, S., Satnami, M. L., & Ghosh, K. K. (2017). A comparative study on the effect of imidazolium-based ionic liquid on self-aggregation of cationic, anionic and nonionic surfactants studied by surface tension, conductivity, fluorescence and FTIR spectroscopy. *Journal of Molecular Liquids*, *241*, 622–632.

Bekhoukh, A., Moulefera, I., Zeggai, F. Z., Benyoucef, A., & Bachari, K. (2021). Anionic methyl orange removal from aqueous solutions by activated carbon reinforced conducting polyaniline as adsorbent: synthesis, characterization, adsorption behavior, regeneration and kinetics study. *Journal of Polymers and the Environment*, 1–10.

Benkhaya, S., M' rabet, S., & El Harfi, A. (2020). A review on classifications, recent synthesis and applications of textile dyes. *Inorganic Chemistry Communications*, *115*, 1–35.

Berradi, M., Hsissou, R., Khudhair, M., Assouag, M., Cherkaoui, O., El Bachiri, A., & El Harfi, A. (2019). Textile finishing dyes and their impact

on aquatic environs. *Heliyon*, *5*(11), 1–11.

Bi, H., Yin, Z., Cao, X., Xie, X., Tan, C., Huang, X., … Zhang, H. (2013). Carbon fiber aerogel made from raw cotton: A novel, efficient and recyclable sorbent for oils and organic solvents. *Advanced Materials*, *25*(41), 5916–5921.

Buchtová, N., & Budtova, T. (2016). Cellulose aero-, cryo- and xerogels: towards understanding of morphology control. *Cellulose*, *23*(4), 2585–2595.

Candido, R. G., & Gonçalves, A. R. (2019). Evaluation of two different applications for cellulose isolated from sugarcane bagasse in a biorefinery concept. *Industrial Crops and Products*, *142*, 1–9.

Chen, Y. X., Sepahvand, S., Gauvin, F., Schollbach, K., Brouwers, H. J. H., & Yu, Q. (2021). One-pot synthesis of monolithic silica-cellulose aerogel applying a sustainable sodium silicate precursor. *Construction and Building Materials*, *293*, 1--13.

Cheruiyot, G. K., Wanyonyi, W. C., Kiplimo, J. J., & Maina, E. N. (2019). Adsorption of toxic crystal violet dye using coffee husks: Equilibrium, kinetics and thermodynamics study. *Scientific African*, *5*, 1–11.

Cihanoğlu, A., & Altinkaya, S. A. (2020). A facile route to the preparation of antibacterial polysulfone-sulfonated polyethersulfone ultrafiltration membranes using a cationic surfactant cetyltrimethylammonium bromide. *Journal of Membrane Science*, *594*, 1–13.

Ciobanu, G., Harja, M., Diaconu, M., Cimpeanu, C., Teodorescu, R., & Bucur, D. (2014). Crystal violet dye removal from aqueous solution by nanohydroxyapatite. *Journal of Food, Agriculture & Environment*, *12*(1), 499–502.

Collazo-Bigliardi, S., Ortega-Toro, R., & Chiralt Boix, A. (2018). Isolation and characterisation of microcrystalline cellulose and cellulose nanocrystals from coffee husk and comparative study with rice husk. *Carbohydrate Polymers*, *191*, 205–215.

Courtenay, J. C., Sharma, R. I., & Scott, J. L. (2018). Recent advances in modified cellulose for tissue culture applications. *Molecules*, *23*(3), 1–20.

Cui, D., Zhang, M., Wang, J., Wang, H., & Zhao, M. (2020). Effect of quinoid redox mediators during azo dye decolorization by anaerobic sludge: Considering the catalyzing mechanism and the methane production. *Ecotoxicology and Environmental Safety*, *202*, 1–8.

Cyril, N., George, J. B., Joseph, L., & Sylas, V. P. (2019). Catalytic degradation of methyl orange and selective sensing of mercury ion in aqueous solutions using green synthesized silver nanoparticles from

the seeds of derris trifoliata. *Journal of Cluster Science*, *30*(2), 459–468.

De Aguiar, J., Bondancia, T. J., Claro, P. I. C., Mattoso, L. H. C., Farinas, C. S., & Marconcini, J. M. (2020). Enzymatic deconstruction of sugarcane bagasse and straw to obtain cellulose nanomaterials. *ACS Sustainable Chemistry and Engineering*, *8*(5), 2287–2299.

de Luna, M. D. G., Flores, E. D., Genuino, D. A. D., Futalan, C. M., & Wan, M. W. (2013). Adsorption of Eriochrome Black T (EBT) dye using activated carbon prepared from waste rice hulls-Optimization, isotherm and kinetic studies. *Journal of the Taiwan Institute of Chemical Engineers*, *44*(4), 646–653.

Dilamian, M., & Noroozi, B. (2020). Rice straw agri-waste for water pollutant adsorption: Relevant mesoporous super hydrophobic cellulose aerogel. *Carbohydrate Polymers*, *251*, 1–13.

Ding, L. P., & Bhatia, S. K. (2003). Analysis of multicomponent adsorption kinetics on activated carbon. *AIChE Jornal*, *49*(4), 883–895.

Dovi, E., Kani, A. N., Aryee, A. A., Jie, M., Li, J., Li, Z., … Han, R. (2021). Decontamination of bisphenol A and Congo red dye from solution by using CTAB functionalised walnut shell. *Environmental Science and Pollution Research*, *28*(22), 28732–28749.

Duhan, M., & Kaur, R. (2020). Adsorptive removal of methyl orange with polyaniline nanofibers: an unconventional adsorbent for water treatment. *Environmental Technology (United Kingdom)*, *41*(23), 2977–2990.

Ekatrisnawan, R. (2016). *Pemanfaatan karbon aktif ampas tebu untuk menurunkan kadar logam Pb dalam larutan air*. *Universitas Negeri Semarang*. Universitas Negeri Semarang.

Fahdil, A., Al-niaimi, D., & Olaiwy, A. A. (2018). Adsorption of Orange G dye from aqueous solutions using magnesium oxide nanoparticles. *Journal of Biochemical Technology*, *9*(3), 31–38.

Fajriutami, T., Fatriasari, W., & Hermiati, E. (2016). Pengaruh pra perlakuan basa pada ampas tebu terhadap karakterisasi pulp dan produksi gula pereduksi. *Jurnal Riset Industri*, *10*(3), 147–161.

Finlay, K. A., Gawryla, M. D., & Schiraldi, D. A. (2015). Effects of fiber reinforcement on clay aerogel composites. *Materials*, *8*(8), 5440–5451.

France, K. J. De, Hoare, T., & Cranston, E. D. (2017). Review of Hydrogels and Aerogels Containing Nanocellulose. *Chemistry of Materials*, *29*, 4609−4631.

Galiwango, E., Abdel Rahman, N. S., Al-Marzouqi, A. H., Abu-Omar, M. M.,

& Khaleel, A. A. (2019). Isolation and characterization of cellulose and α-cellulose from date palm biomass waste. *Heliyon*, *5*(12), 1–8.

Gopakumar, D. A., Arumughan, V., Pottathara, Y. B., Sisanth, K. S., Pasquini, D., Bracic, M., … Khalil, A. (2019). Robust superhydrophobic cellulose nanofiber aerogel for multifunctional environmental applications. *Polymers*, *11*(3), 1–14.

Gu, H., Zhou, X., Lyu, S., Pan, D., Dong, M., Wu, S., … Guo, Z. (2020). Magnetic nanocellulose-magnetite aerogel for easy oil adsorption. *Journal of Colloid and Interface Science*, *560*, 849–856.

Gurav, J. L., Jung, I. K., Park, H. H., Kang, E. S., & Nadargi, D. Y. (2010). Silica aerogel: Synthesis and applications. *Journal of Nanomaterials*, *2010*, 1–11.

Halim, C. E., Abib, K., Tjandra, Y., Yosephi, V., & Wardani, A. K. (2019). Pengaruh persentase PVA-alginat beads terhadap tingkat dekolorisasi. *Chimica et Natura Acta*, *7*(2), 63–68.

Han, Y., Zhang, X., Wu, X., & Lu, C. (2015). Flame retardant, heat insulating cellulose aerogels from waste cotton fabrics by in situ formation of magnesium hydroxide nanoparticles in cellulose gel nanostructures. *ACS Sustainable Chemistry and Engineering*, *3*(8), 1853–1859.

Haounati, R., Ouachtak, H., El Haouti, R., Akhouairi, S., Largo, F., Akbal, F., … Addi, A. A. (2021). Elaboration and properties of a new SDS/CTAB@Montmorillonite organoclay composite as a superb adsorbent for the removal of malachite green from aqueous solutions. *Separation and Purification Technology*, *255*, 1–43.

Hapsoro, D. (2019). *Kultur In Vitro tanaman tebu dan manfaatnya untuk mutagenesis dengan sinar gamma*. Bandar Lampung: Anugrah Utama Raharja.

Hassanzadeh-Tabrizi, S. A., Motlagh, M. M., & Salahshour, S. (2016). Synthesis of ZnO/CuO nanocomposite immobilized on γ-Al2O3 and application for removal of methyl orange. *Applied Surface Science*, *384*, 237–243.

Heinze, T., Seoud, O. A. El, & Koschella, A. (2018). Production and Characteristics of Cellulose from Different Sources. *Cellulose Derivates*, 1–38.

Hidayanti, S., Sugiharto, R., & Zuidar, A. S. (2019). Karakteristik pulp hasil pemutihan dari tandan kosong kelapa sawit hasil pemasakan yang menggunakan limbah lindi hitam siklus ketiga. *Journal of Tropical Upland Resources*, *1*(1), 103–108.

Holtzapple, M. T., & Granda, C. B. (2009). Carboxylate platform: The MixAlco process part 1: Comparison of three biomass conversion

platforms. *Applied Biochemistry and Biotechnology*, *156*, 525–536.

Hou, M., Li, F., Liu, X., Wang, X., & Wan, H. (2007). The effect of substituent groups on the reductive degradation of azo dyes by zerovalent iron. *Journal of Hazardous Materials*, *145*, 305–314.

Hubbe, M. A., Venditti, R. A., & Rojas, O. J. (2007). What happens to cellulosic fibers during papermaking and recycling? A review. *BioResources*, *2*(4), 739–788.

Iqbal, S., Zahoor, C., Musaddiq, S., Hussain, M., Begum, R., Irfan, A., … Farooqi, Z. H. (2020). Silver nanoparticles stabilized in polymer hydrogels for catalytic degradation of azo dyes. *Ecotoxicology and Environmental Safety*, *202*, 1–9.

Istirokhatun, T., Rokhati, N., Rachmawaty, R., Meriyani, M., Priyanto, S., & Susanto, H. (2015). Cellulose isolation from tropical water hyacinth for membrane preparation. *Procedia Environmental Sciences*, *23*, 274–281.

Jamee, R., & Siddique, R. (2019). Biodegradation of synthetic dyes of textile effluent by microorganisms: an environmentally and economically sustainable approach. *European Journal of Microbiology and Immunology*, *9*(4), 114–118.

Jeeva, M., Zuhairi, W., & Yaacob, W. (2018). Comparison study on the adsorption of a synthetic textile dye using bentonite and surfactant modified bentonite. *Bulletin of the Geological Society of Malaysia*, *65*, 107–117.

Jeyajothi, K. (2014). Removal of dyes from textile wastewater usingOrange peel as adsorbent. *Journal of Chemical and Pharmaceutical Sciences*, (4), 161–163.

Jia, Y., Ding, L., Ren, P., Zhong, M., Ma, J., & Fan, X. (2020). Performances and mechanism of methyl orange and congo red adsorbed on the magnetic ion-exchange resin. *Journal of Chemical and Engineering Data*, *65*(2), 725–736.

Jiménez-Saelices, C., Seantier, B., Cathala, B., & Grohens, Y. (2017). Effect of freeze-drying parameters on the microstructure and thermal insulating properties of nanofibrillated cellulose aerogels. *Journal of Sol-Gel Science and Technology*, *84*(3), 475–485.

Jin, L., Sun, Q., Xu, Q., & Xu, Y. (2015). Adsorptive removal of anionic dyes from aqueous solutions using microgel based on nanocellulose and polyvinylamine. *Bioresource Technology*, *197*, 348–355.

Jin, Y., Shi, Z., Xu, G., Yang, H., & Yang, J. (2020). A stepwise pretreatment of sugarcane bagasse by alkaline and hydroxymethyl reagent for bioethanol production. *Industrial Crops and Products*, *145*, 1–8.

Kamatchi, K., Sriram, S., Sangeetha, K., Anuranjani, E., Durairaj, M., & Sabari Girisun, T. C. (2021). Enhanced third-order nonlinear optical properties of methyl orange dye-doped potassium penta borate octa hydrate (MOPPB) single crystals using CW diode laser for optical limiting applications. *Journal of Materials Science: Materials in Electronics*, *32*(11), 15171–15181.

Kani, A. N., Dovi, E., Mpatani, F. M., Li, Z., Han, R., & Qu, L. (2020). Tiger nut residue as a renewable adsorbent for methylene blue removal from solution: Adsorption kinetics, isotherm, and thermodynamic studies. *Desalination and Water Treatment*, *191*, 426–437.

Karp, S. G., Woiciechowski, A. L., Soccol, V. T., & Soccol, S. R. (2013). Pretreatment strategies for delignifications of sugarcane bagasse: A review. *Brazilian Archives of Biology and Technology*, *56*(4), 679–69.

Karthikeyan, P., Elanchezhiyan, S. S. D., Banu, H. A. T., Hasmath Farzana, M., & Park, C. M. (2021). Hydrothermal synthesis of hydroxyapatite-reduced graphene oxide (1D–2D) hybrids with enhanced selective adsorption properties for methyl orange and hexavalent chromium from aqueous solutions. *Chemosphere*, *276*, 1–8.

Kaya, M. (2017). Super absorbent, light, and highly flame retardant cellulose-based aerogel crosslinked with citric acid. *Journal of Applied Polymer Science*, *134*(38), 1–9.

Kaya, M., & Tabak, A. (2020). Recycling of an agricultural bio-waste as a novel cellulose aerogel: a Green chemistry study. *Journal of Polymers and the Environment*, *28*(1), 323–330.

Khac, D., Nian, G., Wei, H., Zhang, X., Ba, Q., Phan-thien, N., & Minh, H. (2020). Methyltrimethoxysilane-coated recycled polyethylene terephthalate aerogels for oil spill cleaning applications. *Materials Chemistry and Physics*, *239*, 1–8.

Khan, A. M., Shafiq, F., Khan, S. A., Ali, S., Ismail, B., Hakeem, A. S., … Khan, A. R. (2019). Surface modification of colloidal silica particles using cationic surfactant and the resulting adsorption of dyes. *Journal of Molecular Liquids*, *274*, 673–680.

Kim, B. Y., Moon, J., Yoo, M. J., Kim, S., Kim, J., & Yang, H. (2021). Surface-modified cellulose nanofibril surfactants for stabilizing oil-in-water emulsions and producing polymeric particles. *Applied Chemistry for Engineering*, *32*(1), 110–116.

Konicki, W., Hełminiak, A., Arabczyk, W., & Mijowska, E. (2018). Adsorption of cationic dyes onto Fe@graphite core–shell magnetic nanocomposite: Equilibrium, kinetics and thermodynamics. *Chemical Engineering Research and Design*, *129*, 259–270.

Kuang, Y., Zhang, X., & Zhou, S. (2020). Adsorption of methylene blue in water onto activated carbon by surfactant modification. *Water (Switzerland)*, *12*(2), 1–19.

Kumar, A., & Jena, H. M. (2017). Adsorption of Cr(VI) from aqueous phase by high surface area activated carbon prepared by chemical activation with ZnCl2. *Process Safety and Environmental Protection*, *109*, 63–71.

Kumari, S., Khan, A. A., Chowdhury, A., Bhakta, A. K., Mekhalif, Z., & Hussain, S. (2020). Efficient and highly selective adsorption of cationic dyes and removal of ciprofloxacin antibiotic by surface modified nickel sulfide nanomaterials: Kinetics, isotherm and adsorption mechanism. *Colloids and Surfaces A: Physicochemical and Engineering Aspects*, *586*, 2–41.

Kusumaningtyas, M. P. (2017). *Analisis struktur nano batu apung lombok menggunakan metode BET (Brunauer-Emmet Teller)*. Institut Teknologi Sepuluh Nopember.

Lafi, R., & Hafiane, A. (2015). Removal of methyl orange (MO) from aqueous solution using cationic surfactants modified coffee waste (MCWs). *Journal of the Taiwan Institute of Chemical Engineers*, *000*, 1–10.

Laksaci, H., Khelifi, A., Belhamdi, B., & Trari, M. (2018). The use of prepared activated carbon as adsorbent for the removal of orange G from aqueous solution. *Microchemical Journal*, *145*, 908–913.

Langmuir, I. (1918). The adsorption of gases on plane surfaces of glass, mica and platinum. *Journal of the American Chemical Society*, *40*(9), 467–475.

Lavarack, B. P., Griffin, G. J., & Rodman, D. (2002). The acid hydrolysis of sugarcane bagasse hemicellulose to produce xylose, arabinose, glucose and other products. *EnergyBiomass and Bioenergy*, *23*(5), 367–380.

Lehninger, A. (1994). *Dasar-dasar biokimia*. Jakarta: Erlangga.

Li, H., Wu, S., Du, C., Zhong, Y., & Yang, C. (2020). Preparation, performances, and mechanisms of microbial flocculants for wastewater treatment. *International Journal of Environmental Research and Public Health*, *17*, 1–20.

Li, T., Liu, Y., Wang, T., Wu, Y., He, Y., Yang, R., & Zheng, S. (2018). Microporous and mesoporous materials regulation of the surface area and surface charge property of MOFs by multivariate strategy : Synthesis , characterization , selective dye adsorption and separation. *Microporous and Mesoporous Materials*, *272*, 101–108.

Li, V. C. F., Dunn, C. K., Zhang, Z., Deng, Y., & Qi, H. J. (2017). Direct ink

write (DIW) 3D printed cellulose nanocrystal aerogel structures. *Scientific Reports*, *7*(1), 1–8.

Li, Z., Hu, J., Xiao, Y., Zha, Q., Zeng, L., & Zhu, M. (2021). Surfactant assisted Cr-metal organic framework for the detection of bisphenol A in dust from E-waste recycling area. *Analytica Chimica Acta*, *1146*, 174–183.

Liebner, F., Potthast, A., Rosenau, T., Haimer, E., & Wendland, M. (2007). Ultralight-eeight cellulose aerogels from NBnMO-stabilized lyocell dopes. *Research Letters in Materials Science*, *2007*, 1–4.

Lin, J., Yu, L., Tian, F., Zhao, N., Li, X., Bian, F., & Wang, J. (2014). Cellulose nanofibrils aerogels generated from jute fibers. *Carbohydrate Polymers*, *109*, 35–43.

Liu, P., Sehaqui, H., Tingaut, P., Wichser, A., Oksman, K., & Mathew, A. P. (2014). Cellulose and chitin nanomaterials for capturing silver ions (Ag+) from water via surface adsorption. *Cellulose*, *21*(1), 449–461.

Liu, Q., Lu, Y., Aguedo, M., Jacquet, N., Ouyang, C., He, W., … Richel, A. (2017). Isolation of high-purity cellulose nanofibers from wheat straw through the combined environmentally friendly methods of steam explosion, microwave-assisted hydrolysis, and microfluidization. *ACS Sustainable Chemistry and Engineering*, *5*(7), 6183–6191.

Liu, S., Yu, T., Hu, N., Liu, R., & Liu, X. (2012). High strength cellulose aerogels prepared by spatially confined synthesis of silica in bioscaffolds. *Colloids and Surfaces A: Physicochemical and Engineering Aspects*, *439*, 159–166.

Long, L. Y., Weng, Y. X., & Wang, Y. Z. (2018). Cellulose aerogels: Synthesis, applications, and prospects. *Polymers*, *8*(6), 1–28.

Ma, Y. zhi, Zheng, D. feng, Mo, Z. ye, Dong, R. jing, & Qiu, X. qing. (2018). Magnetic lignin-based carbon nanoparticles and the adsorption for removal of methyl orange. *Colloids and Surfaces A: Physicochemical and Engineering Aspects*, *559*, 226–234.

Mani, S., & Bharagava, R. N. (2016). Exposure to crystal violet, its toxic, genotoxic and carcinogenic effects on environment and its degradation and detoxification for environmental safety. *Reviews of Environmental Contamination and Toxicology*, *237*, 71–104.

Mansor, E. S., Ali, H., & Abdel-Karim, A. (2020). Efficient and reusable polyethylene oxide/polyaniline composite membrane for dye adsorption and filtration. *Colloids and Interface Science Communications*, *39*, 1–12.

Mapukata, S., Kobayashi, N., Kimura, M., & Nyokong, T. (2019). Asymmetrical and symmetrical zinc phthalocyanine-cobalt ferrite

conjugates embedded in electrospun fibers for dual photocatalytic degradation of azo dyes: Methyl Orange and Orange G. *Journal of Photochemistry and Photobiology A: Chemistry*, *379*, 112–122.

Meneses, I. P., Novaes, S. D., Dezotti, R. S., Oliveira, P. V., & Petri, D. F. S. (2022). CTAB-modified carboxymethyl cellulose/bagasse cryogels for the efficient removal of bisphenol A, methylene blue and Cr(VI) ions: Batch and column adsorption studies. *Journal of Hazardous Materials*, *421*, 1–17.

Menezes, D. B., Diz, F. M., Romanholo Ferreira, L. F., Corrales, Y., Baudrit, J. R. V., Costa, L. P., & Hernández-Macedo, M. L. (2021). Starch-based biocomposite membrane reinforced by orange bagasse cellulose nanofibers extracted from ionic liquid treatment. *Cellulose*, *28*(7), 4137–4149.

Miao, Y., Pudukudy, M., Zhi, Y., Miao, Y., Shan, S., Jia, Q., & Ni, Y. (2020). A facile method for in situ fabrication of silica/cellulose aerogels and their application in CO2 capture. *Carbohydrate Polymers*, *236*.

Mirzaei, D., Zabardasti, A., Mansourpanah, Y., Sadeghi, M., & Farhadi, S. (2020). Efficacy of novel NaX/MgO–TiO2 zeolite nanocomposite for the adsorption of methyl orange (MO) dye: isotherm, kinetic and thermodynamic Studies. *Journal of Inorganic and Organometallic Polymers and Materials*, *30*(6), 2067–2080.

Mobarak, M., Mohamed, E. A., Selim, A. Q., Mohamed, F. M., Sellaoui, L., Bonilla-Petriciolet, A., & Seliem, M. K. (2019). Statistical physics modeling and interpretation of methyl orange adsorption on high–order mesoporous composite of MCM–48 silica with treated rice husk. *Journal of Molecular Liquids*, *285*, 678–687.

Mobarak, M., Selim, A. Q., Mohamed, E. A., & Seliem, M. K. (2018). A superior adsorbent of CTAB/H2O2 solution−modified organic carbon rich-clay for hexavalent chromium and methyl orange uptake from solutions. *Journal of Molecular Liquids*, *259*(2017), 384–397.

Mosier, N. S., Ladisch, C. M., & Ladisch, M. R. (2002). Characterization of acid catalytic domains for cellulose hydrolysis and glucose degradation. *Biotechnology and Bioengineering*, *79*(6), 610–618.

Mozetič, M. (2019). Surface modification to improve properties of materials. *Materials*, *12*(3), 2–8.

Nabi, A., Tasneem, S., Jesudason, C. G., Lee, V. S., & Zain, S. B. M. (2018). Study of interaction between cationic surfactant (CTAB) and paracetamol by electrical conductivity, tensiometric and spectroscopic methods. *Journal of Molecular Liquids*, *256*, 100–107.

Naushad, M., Alqadami, A. A., AlOthman, Z. A., Alsohaimi, I. H., Algamdi,

M. S., & Aldawsari, A. M. (2019). Adsorption kinetics, isotherm and reusability studies for the removal of cationic dye from aqueous medium using arginine modified activated carbon. *Journal of Molecular Liquids*, *293*, 1–8.

Nazir, M. A., Khan, N. A., Cheng, C., Shah, S. S. A., Najam, T., Arshad, M., … Rehman, A. ur. (2020). Surface induced growth of ZIF-67 at Co-layered double hydroxide: Removal of methylene blue and methyl orange from water. *Applied Clay Science*, *190*, 1–9.

Nguyen, S. T., Feng, J., Ng, S. K., Wong, J. P. W., Tan, V. B. C., & Duong, H. M. (2014). Advanced thermal insulation and absorption properties of recycled cellulose aerogels. *Colloids and Surfaces A: Physicochemical and Engineering Aspects*, *445*, 128–134.

Nunes, L. J. R., Loureiro, L. M. E. F., Sá, L. C. R., & Silva, H. F. C. (2020). Sugarcane industry waste recovery: A case study using thermochemical conversion technologies to increase sustainability. *Applied Sciences (Switzerland)*, *10*(18), 2–17.

Pei, R., Li, Q., Liu, J., Yang, G., Wu, Q., Wu, M., … Liu, M. (2020). Adsorption/reduction behaviors of modified cellulose aerogels for the removal of low content of Cr(VI). *Journal of Polymers and the Environment*, *28*(8), 2199–2210.

Pérez-calderón, J., Santos, M. V., & Zaritzky, N. (2020). Synthesis, characterization and application of cross-linked chitosan/oxalic acid hydrogels to improve azo dye (Reactive Red 195) adsorption. *Reactive and Functional Polymers*, *155*, 1–14.

Piaskowski, K., Świderska-Dąbrowska, R., & Zarzycki, P. K. (2018). Dye removal from water and wastewater using various physical, chemical, and biological processes. *Journal of AOAC International*, *101*(5), 1371–1384.

Poletto, M., Ornaghi Júnior, H. L., & Zattera, A. J. (2014). Native cellulose: Structure, characterization and thermal properties. *Materials*, *7*(9), 6105–6119.

Popoola, L. T., Aderibigbe, T. A., Yusuff, A. S., & Munir, M. M. (2018). Brilliant green dye adsorption onto composite snail shell–rice husk: Adsorption isotherm, kinetic, mechanistic, and thermodynamics analysis. *Environmental Quality Management*, *28*(2), 63–78.

Purwaningsih, H., Ervianto, Y., Pratiwi, V. M., Susanti, D., & Purniawan, A. (2019). Effect of cetyl trimethyl ammonium bromide as template of mesoporous silica MCM-41 from rice husk by sol-gel method. *IOP Conference Series: Materials Science and Engineering*, *515*(1), 0–9.

Qu, J., Yuan, Z., Wang, C., Wang, A., Liu, X., Wei, B., & Wen, Y. (2019).

Enhancing the redispersibility of TEMPO-mediated oxidized cellulose nanofibrils in N,N-dimethylformamide by modification with cetyltrimethylammonium bromide. *Cellulose*, *26*, 7769–7780.

Rajasimman, M., Babu, S. V., & Rajamohan, N. (2017). Biodegradation of textile dyeing industry wastewater using modified anaerobic sequential batch reactor – Start-up, parameter optimization and performance analysis. *Journal of the Taiwan Institute of Chemical Engineers*, *72*, 171–181.

Ranganagowda, R. P. G., Kamath, S. S., & Bennehalli, B. (2019). Extraction and characterization of cellulose from natural areca fiber. *Material Science Research India*, *16*(1), 86–93.

Ranjbar, D., Raeiszadeh, M., Lewis, L., Maclachlan, M. J., & Hatzikiriakos, S. G. (2020). Adsorptive removal of Congo red by surfactant modified cellulose nanocrystals : a kinetic, equilibrium, and mechanistic investigation. *Cellulose*, *27*, 3211–3232.

Rashid, S., Shahi, A. K., Dutta, H., & Sahu, J. K. (2022). Extraction and characterization of cellulose and cellulose nanowhiskers from almond shell biomass, metal removal and toxicity analysis. *Biointerface Research in Applied Chemistry*, *12*(2), 1705–1720.

Rattanapan, S., Srikram, J., & Kongsune, P. (2017). Adsorption of methyl orange on coffee grounds activated carbon. *Energy Procedia*, *138*, 949–954.

Rubai, H. F. Al, Hassan, A. K., Sultan, M. S., & Abood, W. M. (2021). Kinetics of adsorption of reactive red 120 using bentonite modified by CTAB and study the effect of salts. *Nature Environment and Pollution Technology*, *20*(1), 281–289.

Safaria, S., Idiawati, N., & Zaharah, T. A. (2013). Efektivitas campuranenzim selulase dari Aspergillus niger dan Trichoderma reesei dalam menghidrolisis sustrat sabut kelapa. *JKK*, *37*(1), 359–364.

Şahin, İ., Özbakır, Y., İnönü, Z., Ulker, Z., & Erkey, C. (2018). Kinetics of Supercritical Drying of Gels. *Gels*, *4*(3), 1–29.

Sai, H., Zhang, J., Jin, Z., Fu, R., Wang, M., Wang, Y., … Ma, L. (2020). Robust silica-cellulose composite aerogels with a nanoscale interpenetrating network structure prepared using a streamlined process. *Polymers*, *12*(4).

Samsuri, M, Gozan, M., Mardias, R., Baiquni, M., Hermansyah, H., Wijanarko, A., … Nasikin, M. (2007). Pemanfaatan sellulosa bagas untuk produksi ethanol melalui sakarifikasi dan fermentasi serentak dengan enzim xylanase. *Makara*, *11*(1), 17–24.

Samsuri, Muhammad, Gozan, M., Hermansyah, H., Prasetya, B., Nasikin,

M., & Watanabe, T. (2008). Ethanol production from bagasse with combination of cellulase-cellubiase in simultaneous saccharification and fermentation (SSF) using white rot fungi pre-treatment. *Journal of Chemical and Natural Resources Engineering*, *3*, 20–32.

Sanguanwong, A., Pavasant, P., Jarunglumlert, T., Nakagawa, K., Flood, A., & Prommuak, C. (2020). Hydrophobic cellulose aerogel from waste napkin paper for oil sorption applications. *Nordic Pulp and Paper Research Journal*, *35*(1), 137–147.

Sankhla, S., Sardar, H. H., & Neogi, S. (2021). Greener extraction of highly crystalline and thermally stable cellulose micro-fibers from sugarcane bagasse for cellulose nano-fibrils preparation. *Carbohydrate Polymers*, *251*, 1–9.

Sari, R. A., Firdaus, M. L., & Elvia, R. (2017). Penentuan kesetimbangan, termodinamika dan kinetika adsorpsi arang aktif tempurung kelapa sawit pada zat warna Reactive red dan Direct blue. *Jurnal Pendidikan Dan Ilmu Kimia*, *1*(1), 10–14.

Sawasdee, S., Suwanputra, S., Seesaiya, C., Sritotesporn, S., Tosri, N., Sawangsup, N., … Watcharabundit, P. (2020). Application of agricultural waste activated carbon prepared from sugarcane leaves for methyl orange removal in aqueous solution. *Ood and Applied Bioscience Journal*, *8*(3), 1–18.

Shabbir, S., Faheem, M., Ali, N., Kerr, P. G., & Wu, Y. (2017). Periphyton biofilms: A novel and natural biological system for the effective removal of sulphonated azo dye methyl orange by synergistic mechanism. *Chemosphere*, *167*, 236–246.

Shayesteh, H., Raji, F., & Kelishami, A. R. (2021). Influence of the alkyl chain length of surfactant on adsorption process: A case study. *Surfaces and Interfaces*, *22*, 1–10.

Shettigar, R. R., Misra, N. M., & Patel, K. (2018). Cationic surfactant (CTAB) a multipurpose additive in polymer-based drilling fluids. *Journal of Petroleum Exploration and Production Technology*, *8*(2), 597–606.

Silva, C. E. de F., Gama, B. M. V. da, Gonçalves, A. H. da S., Medeiros, J. A., & Abud, A. K. de S. (2020). Basic-dye adsorption in albedo residue: Effect of pH, contact time, temperature, dye concentration, biomass dosage, rotation and ionic strength. *Journal of King Saud University - Engineering Sciences*, *32*(6), 351–359.

Siregar, M. Y., Lalasari, L. H., Oediyani, S., Irawan, J., Andriyah, L., Arini, T., & Firdiyono, F. (2019). Investigasi model isoterm adsorpsi litium dari brine water-Bogor menggunakan adsrben hydros manganese oxide (HMO) dengan variasi dosis adsorben dan waktu adsorpsi. *Metalurgi*, *3*, 141–150.

Song, Y., Zhou, S., Li, H., Xie, F., Yang, H., Yuan, Z., & Li, W. (2021). Controllable synthesis of cellulose/methylene bisacrylamide aerogels for enhanced adsorption performance. *Journal of Applied Polymer Science*, *138*(15), 1–9.

Statistik, B. P. (2021). *Statistik Tebu Indonesia 2020*.

Subbaiah, M. V., & Kim, D. S. (2016). Adsorption of methyl orange from aqueous solution by aminated pumpkin seed powder: Kinetics, isotherms, and thermodynamic studies. *Ecotoxicology and Environmental Safety*, *128*, 109–117.

Sudha, M., Saranya, A., Selvakumar, G., & Sivakumar, N. (2014). Microbial degradation of Azo Dyes: A review. *International Journal Current Microbiology and Applied Sciences*, *3*(2), 670–690.

Sulyman, M., Kucinska-Lipka, J., Sienkiewicz, M., & Gierak, A. (2021). Development, characterization and evaluation of composite adsorbent for the adsorption of crystal violet from aqueous solution: Isotherm, kinetics, and thermodynamic studies. *Arabian Journal of Chemistry*, *14*(5), 1–16.

Sulyman, M., Namieśnik, J., & Gierak, A. (2016). Adsorptive removal of aqueous phase crystal violet dye by low-cost activated carbon obtained from date palm (L.) dead leaflets. *Engineering and Protection of Environment*, *19*(4), 611–631.

Sun, X., Zhou, Y., & Zheng, X. (2020). Comparison of adsorption behaviors of Fe-La oxides co-loaded MgO nanosheets for the removal of methyl orange and phosphate in single and binary systems. *Journal of Environmental Chemical Engineering*, *8*(5).

Takeuchi, H., Higashitani, S., Nagai, K., Choi, H. C., Moon, B. H., Masuhara, N., … Mulders, N. (2012). Knudsen-to-hydrodynamic crossover in liquid He3 in a high-porosity aerogel. *Physical Review Letters*, *108*(22), 1–5.

Tang, C., Brodie, P., Li, Y., Grishkewich, N. J., Brunsting, M., & Tam, K. C. (2020). Shape recoverable and mechanically robust cellulose aerogel beads for efficient removal of copper ions. *Chemical Engineering Journal*, *392*, 1–11.

Tang, M., Jia, R., Kan, H., Liu, Z., Yang, S., Sun, L., & Yang, Y. (2020). Kinetic, isotherm, and thermodynamic studies of the adsorption of dye from aqueous solution by propylene glycol adipate-modified cellulose aerogel. *Colloids and Surfaces A: Physicochemical and Engineering Aspects*, *602*, 1–23.

Tao, P., Zhang, Y., Wu, Z., Liao, X., & Nie, S. (2019). Enzymatic pretreatment for cellulose nanofibrils isolation from bagasse pulp: Transition of cellulose crystal structure. *Carbohydrate Polymers*, *214*,

1–7.

Tarkwa, J. B., Oturan, N., Acayanka, E., Laminsi, S., & Oturan, M. A. (2019). Photo-Fenton oxidation of Orange G azo dye: process optimization and mineralization mechanism. *Environmental Chemistry Letters*, *17*(1), 473–479.

Tayeb, A. H., Amini, E., Ghasemi, S., & Tajvidi, M. (2018). Cellulose nanomaterials-binding properties and applications: A review. *Molecules*, *23*(10), 1–24.

Thai, Q. B., Nguyen, S. T., Ho, D. K., Tran, T. Du, Huynh, D. M., Do, N. H. N., … Duong, H. M. (2020). Cellulose-based aerogels from sugarcane bagasse for oil spill-cleaning and heat insulation applications. *Carbohydrate Polymers*, *228*, 1–7.

Timmer, N., Gore, D., Sanders, D., Gouin, T., & Droge, S. T. J. (2019). Toxicity mitigation and bioaccessibility of the cationic surfactant cetyltrimethylammonium bromide in a sorbent-modified biodegradation study. *Chemosphere*, *222*, 461–468.

Tran, V. A., Kadam, A. N., & Lee, S. W. (2020). Adsorption-assisted photocatalytic degradation of methyl orange dye by zeolite-imidazole-framework-derived nanoparticles. *Journal of Alloys and Compounds*, *835*, 1–10.

Walas, S. M. (1990). *Chemical process equipment*. United States of America: Butterworth-Heinemann.

Wan, C., Lu, Y., Jiao, Y., Cao, J., Sun, Q., & Li, J. (2015). Preparation of mechanically strong and lightweight cellulose aerogels from Preparation of mechanically strong and lightweight cellulose aerogels from cellulose-NaOH / PEG solution. *Journal of Sol-Gel Science and Technology*, *74*(1), 2–5.

Wang, G., Huang, R., Zhou, A., & Xu, Q. (2019). Degradation of methyl orange by a new catalyst glyphosate ferrous. *Solid State Sciences*, *95*, 1–5.

Wang, X., Deng, B., Yu, L., Cui, E., Xiang, Z., & Lu, W. (2020). Degradation of azo dyes Congo red by MnBi alloy powders: Performance, kinetics and mechanism. *Materials Chemistry and Physics*, *251*, 1–7.

Wang, Y., Zhao, L., Hou, J., Peng, H., Wu, J., Liu, Z., & Guo, X. (2018). Kinetic, isotherm, and thermodynamic studies of the adsorption of dyes from aqueous solution by cellulose-based adsorbents. *Water Science and Technology*, *77*(11), 2699–2708.

Widia, I., & Wathoni, N. (2014). Review artikel selulosa mikrokristal: isolasi, karakterisasi dan aplikasi dalam bidang farmasetik. *Jurnal Farmaka*, *15*(2), 127–143.

Wijayanti, I. E., & Kurniawati, E. A. (2019). Studi kinetika adsorpsi isoterm persamaan Langmuir dan Freundlich pada abu gosok sebagai adsorben. *EduChemia (Jurnal Kimia Dan Pendidikan)*, *4*(2), 175–184.

Wu, L., Liu, X., Lv, G., Zhu, R., Tian, L., Liu, M., … Liao, L. (2021). Study on the adsorption properties of methyl orange by natural one-dimensional nano-mineral materials with different structures. *Scientific Reports*, *11*(1), 1–11.

Wu, Y., Su, M., Chen, J., Xu, Z., Tang, J., Chang, X., & Chen, D. (2019). Superior adsorption of methyl orange by h-MoS2 microspheres: Isotherm, kinetics, and thermodynamic studies. *Dyes and Pigments*, *170*, 1–8.

Xu, A. R., Wang, J. J., & Guo, X. (2018). Fabrication of cellulose aerogels using a green/clean procedure. *Journal of Macromolecular Science, Part B: Physics*, *57*(1), 1–7.

Yang, J., & Li, J. (2018). Self-assembled cellulose materials for biomedicine: A review. *Carbohydrate Polymers*, *181*, 264–274.

Yang, X., Wang, X., Liu, H., Zhao, Y., Jiang, S., & Liu, L. (2016). Impact of dimethyl sulfoxide treatment on morphology and characteristics of nanofibrillated cellulose isolated from corn husks. *BioResources*, *12*(1), 95–106.

Yang, Y., Yang, J., Du, Y., Li, C., Wei, K., Lu, J., … Yang, L. (2019). Preparation and characterization of cationic water-soluble pillar[5]arene-modified zeolite for adsorption of methyl orange. *ACS Omega*, *4*(18), 17741–17751.

Yaseen, D. A., & Scholz, M. (2019). *Textile dye wastewater characteristics and constituents of synthetic effluents : a critical review*. *International Journal of Environmental Science and Technology* (Vol. 16). Springer Berlin Heidelberg.

Yönten, V., Sanyürek, N. K., & Kivanç, M. R. (2020). A thermodynamic and kinetic approach to adsorption of methyl orange from aqueous solution using a low cost activated carbon prepared from Vitis vinifera L. *Surfaces and Interfaces*, *20*, 1–8.

Youssef, N. A., Shaban, S. A., Ibrahim, F. A., & Mahmoud, A. S. (2016). Degradation of methyl orange using Fenton catalytic reaction. *Egyptian Journal of Petroleum*, *25*(3), 317–321.

Yu, J., Zhang, X., Wang, D., & Li, P. (2018). Adsorption of methyl orange dye onto biochar adsorbent prepared from chicken manure. *Water Science and Technology*, *77*(5), 1303–1312.

Yu, Y., Qiao, N., Wang, D., Zhu, Q., Fu, F., Cao, R., … Xu, B. (2019). Fluffy honeycomb-like activated carbon from popcorn with high surface area

and well-developed porosity for ultra-high efficiency adsorption of organic dyes. *Bioresource Technology*, *285*, 1–10.

Yunus, M. A. (2019). *Sintesis aerogel selulosa dari sekam padi serta aplikasinya pada penyerapan metilen biru*. *Tesis*. Universitas Hasanuddin.

Yuvaraja, G., Chen, D. Y., Pathak, J. L., Long, J., Subbaiah, M. V., Wen, J. C., & Pan, C. L. (2020). Preparation of novel aminated chitosan schiff's base derivative for the removal of methyl orange dye from aqueous environment and its biological applications. *International Journal of Biological Macromolecules*, *146*, 1100–1110.

Zhai, L., Bai, Z., Zhu, Y., Wang, B., & Luo, W. (2018). Fabrication of chitosan microspheres for efficient adsorption of methyl orange. *Chinese Journal of Chemical Engineering*, *26*(3), 657–666.

Zhang, C., Uchikoshi, T., Ichinose, I., & Liu, L. (2019). Surface modification on cellulose nanofibers by TiO2 coating for achieving high capture efficiency of nanoparticles. *Coatings*, *9*(2).

Zhang, Z., Zhu, M., & Zhang, D. (2018). A Thermogravimetric study of the characteristics of pyrolysis of cellulose isolated from selected biomass. *Applied Energy*, *220*, 87–93.

Zhao, Y., Sun, B., Wang, T., Yang, L., Xu, X., Chen, C., … Sun, D. (2020). Synthesis of cellulose–silica nanocomposites by in situ biomineralization during fermentation. *Cellulose*, *27*(2), 703–712.

Zhou, Y., Fu, S., Pu, Y., Pan, S., & Ragauskas, A. J. (2014). Preparation of aligned porous chitin nanowhisker foams by directional freeze-casting technique. *Carbohydrate Polymers*, *112*, 277–283.

Zhu, W., Jiang, X., Liu, F., You, F., & Yao, C. (2020). Preparation of chitosan-graphene oxide composite aerogel by hydrothermal method and its adsorption property of methyl orange. *Polymers*, *12*(9), 1–16.

Zubair, M., Jarrah, N., Khalid, A., & Saood, M. (2018). Starch-NiFe-layered double hydroxide composites : Ef fi cient removal of methyl orange from aqueous phase. *Journal of Molecular Liquids*, *249*, 254–264.

LAMPIRAN

Lampiran 1. Skema Prosedur Kerja

1. Preparasi Sampel

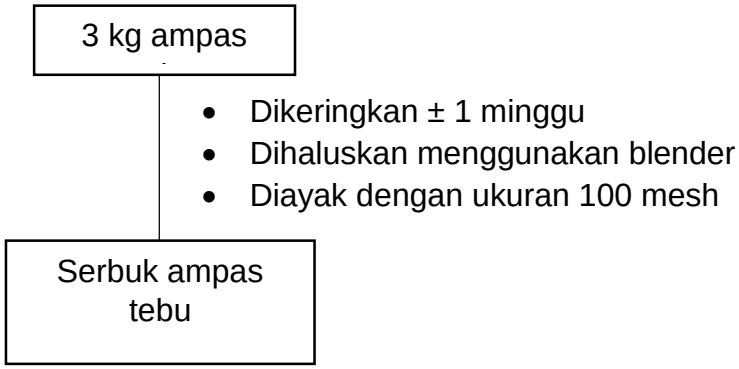

2. Ekstraksi Selulosa

a. Delignifikasi

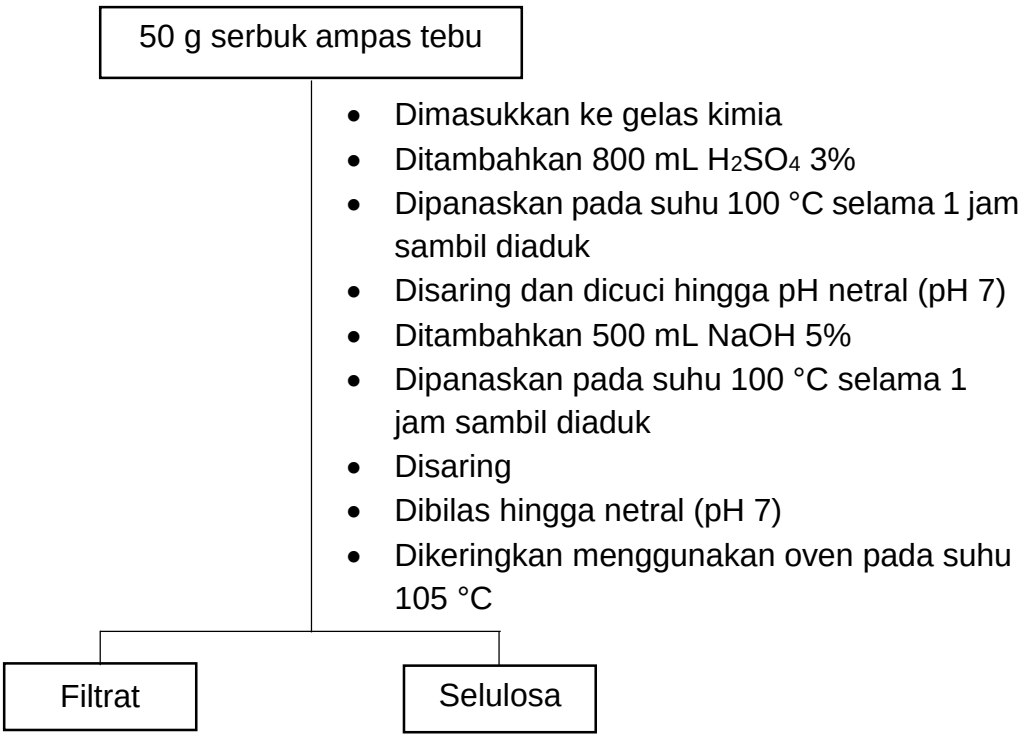

b. *Bleaching*

Selulosa

- Ditambahkan H_2O_2 3% (1:10)
- Dipanaskan suhu 70 °C selama 1 jam sambil diaduk
- Disaring dan dibilas hingga netral (pH 7)
- Dikeringkan dalam oven pada suhu 105 °C
- Ditimbang

Selulosa

3. Pembuatan Aerogel Selulosa

Selulosa

- Dimasukkan ke dalam gelas kimia
- Ditambahkan 20 mL ludox
- Ditambahkan NaOH:Urea (1,9 wt%-10 wt%) 1:5
- Disonikasi selama 6 menit
- Dimasukkan ke dalam freezer selama 24 jam
- Dibiarkan pada suhu kamar
- Direndam dengan 20 mL etanol 99% selama 4 jam
- Direndam dalam aquabides selama 48 jam
- Dimasukkan ke dalam freezer ± -12 °C hingga selama 12 jam
- Dilakukan pengeringan menggunakan freeze-dryer pada suhu -98 °C selama 12 jam

Aerogel Selulosa

- Dikarakterisasi dengan FTIR, XRD, SEM dan luas permukaan dengan metode metilen biru

Hasil karakterisasi

4. Modifikasi Aerogel Selulosa dengan CTAB

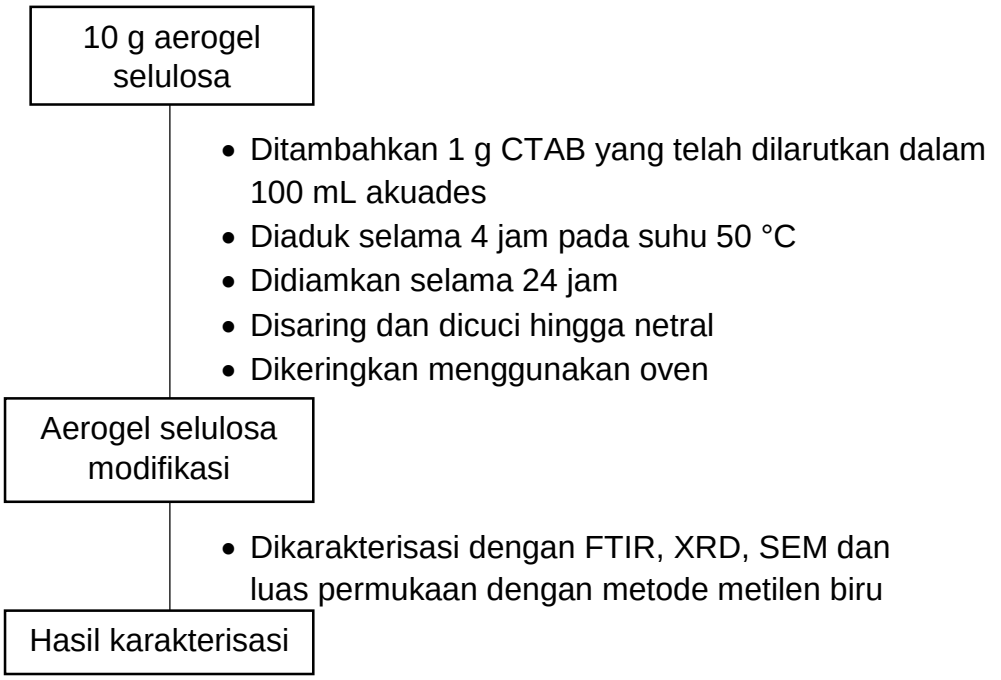

5. Luas Permukaan dengan Metiln Biru

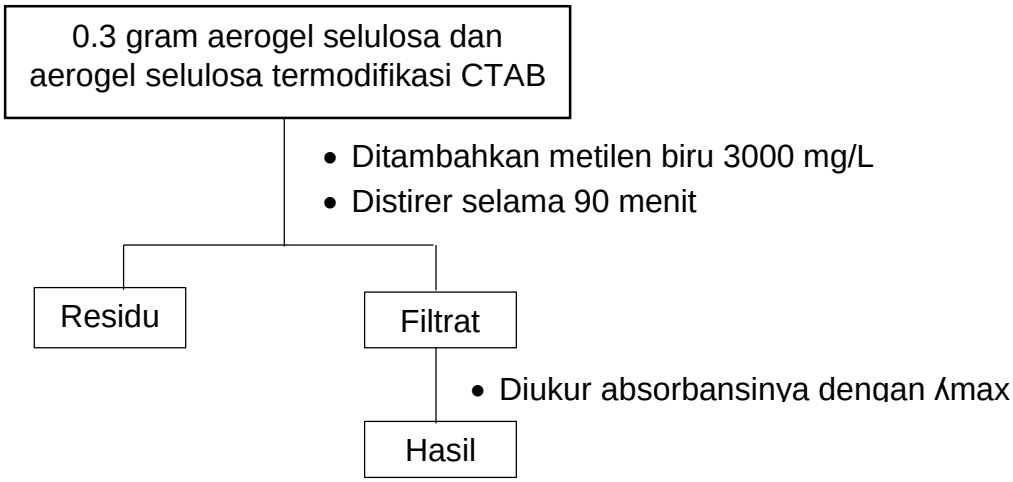

6. Kondisi Optimum Adsorpsi *Methyl orange*

a. Waktu kontak optimum

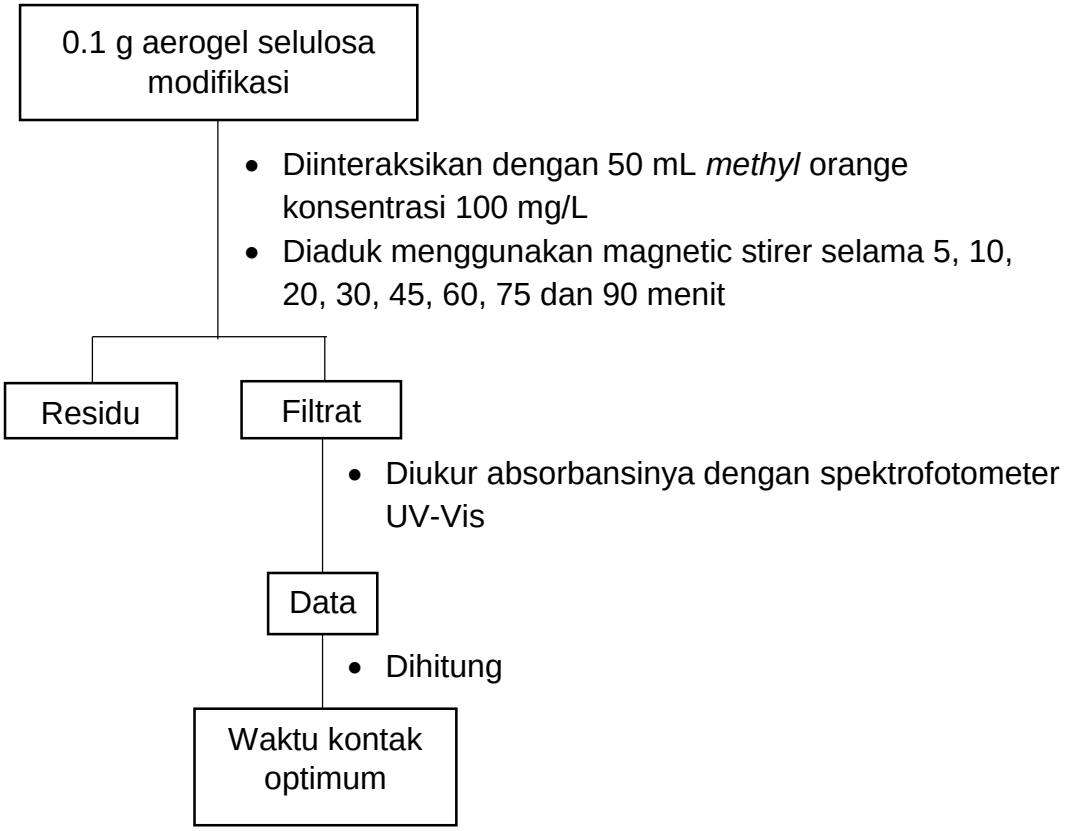

b. Suhu optimum

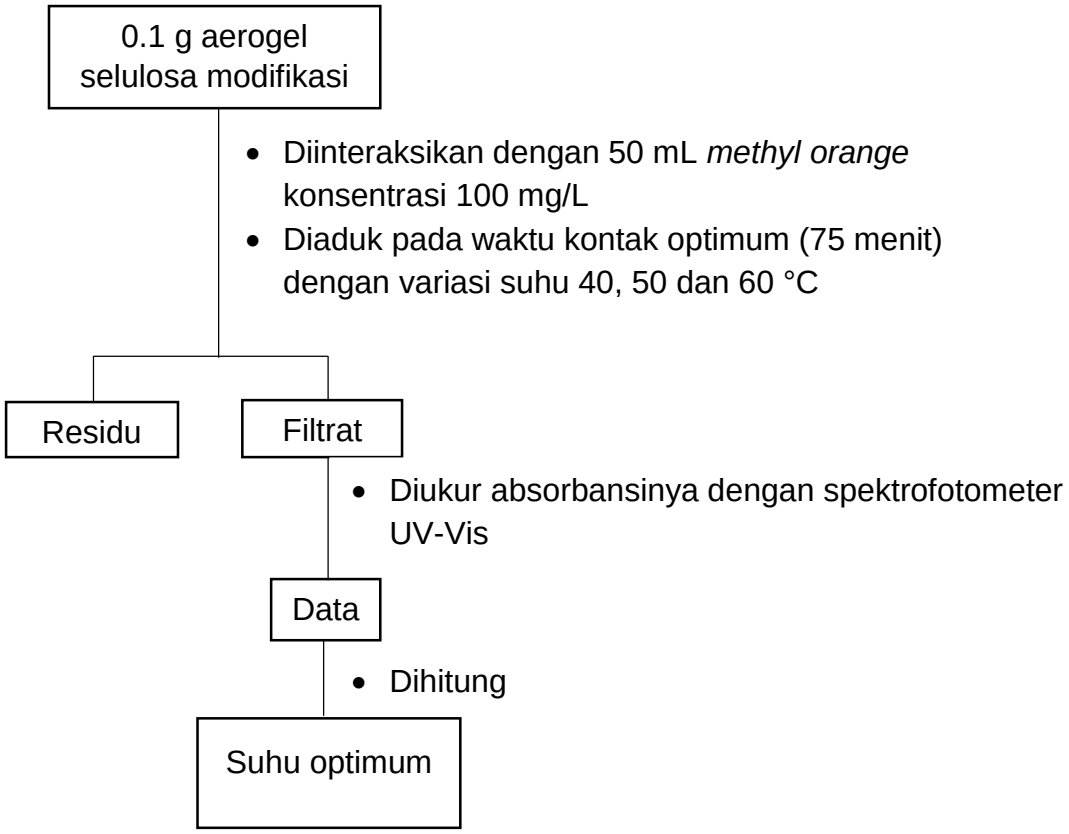

c. Pengaruh Konsentrasi

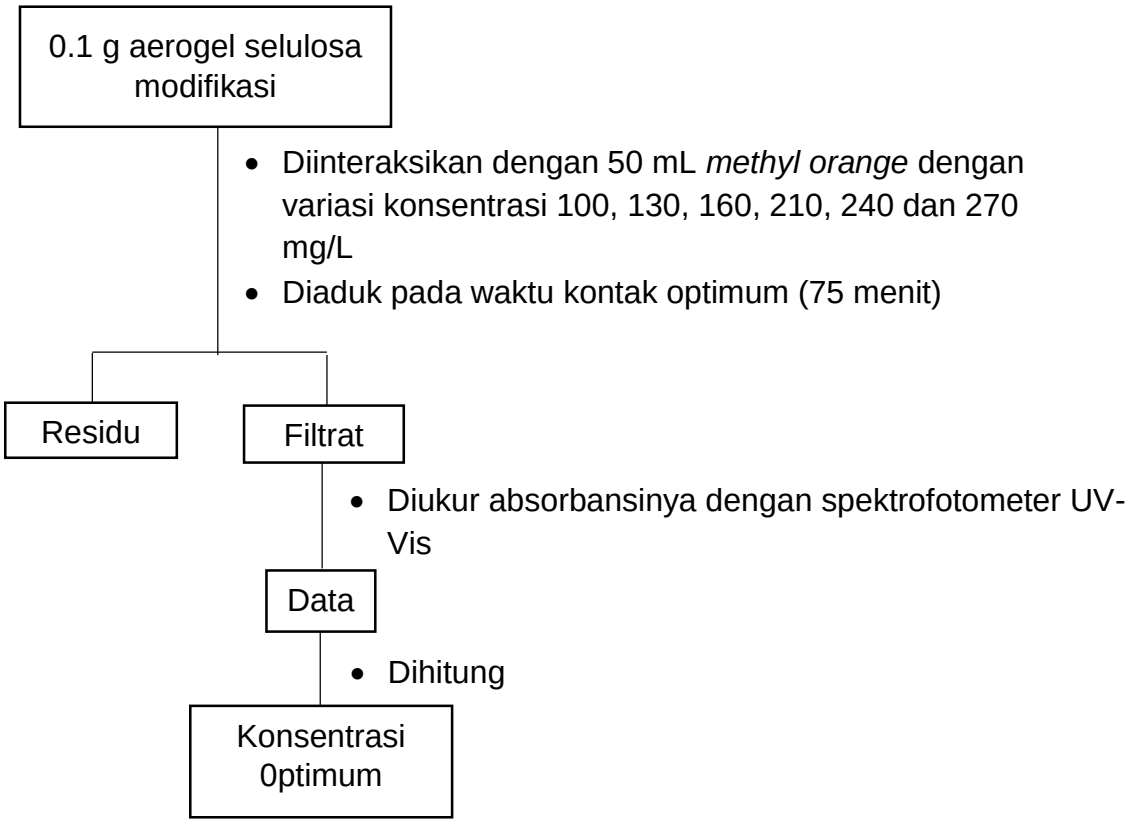

Lampiran 2. Dokumentasi Kegiatan Penelitian

- **Preparasi Sampel**

Gambar 1. Sampel ampas tebu

Gambar 2. Sampel ampas tebu yang berukuran 100 mesh

- **Ekstraksi Ampas Tebu**
  - Delignifikasi

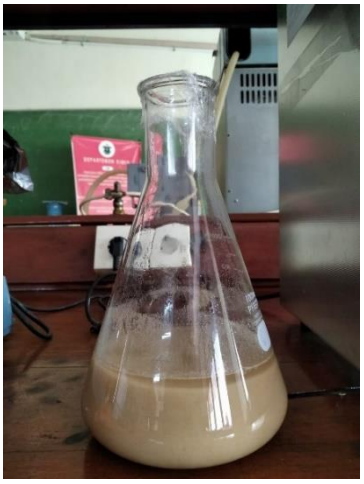

Gambar 3. Ampas tebu ditambahkan H_2SO_4

Gambar 4. Ampas tebu + H_2SO_4 setelah dipanaskan

Gambar 5. Proses penyaringan dan pencucian hingga netral

Gambar 6. Residu ekstraksi ampas tebu dengan H_2SO_4

Gambar 7. Residu + NaOH dan dipanaskan

Gambar 8. Proses penyaringan dan pencucian hingga netral

Gambar 9. Residu hasil delignifikasi

- Bleaching

Gambar 10. Residu hasil delignifikasi + H_2O_2 dan dipanaskan

Gambar 11. Residu hasil bleaching

- **Sintesis Aerogel Selulosa**

Gambar 11. Selulosa + ludox + NaOH-Urea

Gambar 12. Proses sonikasi

Gambar 13. Setelah di *freezer* dan pencairan pada suhu kamar

Gambar 14. Aerogel selulosa setelah di *freeze drying*

- **Modifikasi Aerogel Selulosa dengan CTAB**

Gambar 15. Aerogel selulosa + CTAB di stirrer dan panaskan suhu 50 °C

Gambar 16. Pendiaman selama 24 jam

Gambar 18. Proses penyaringan dan pencucian hingga netral

Gambar 19. Aerogel selulosa termodifikasi

- **Waktu Kontak Optimum**

Gambar 20. Proses adsorpsi penentuan waktu kontak

Gambar 21. Hasil zat warna setelah disaring

- **Suhu Optimum**

Gambar 22. Proses adsorpsi pada suhu 40, 50 dan 60 °C

Gambar 23. Hasil zat warna setelah disaring

- **Kapasitas Adsorpsi**

Gambar 24. Larutan untuk proses kapasitas adsorpsi

Gambar 24. Hasil zat warna setelah disaring

Lampiran 3. Hasil karakterisasi dengan FTIR

- Hasil FTIR Ampas Tebu

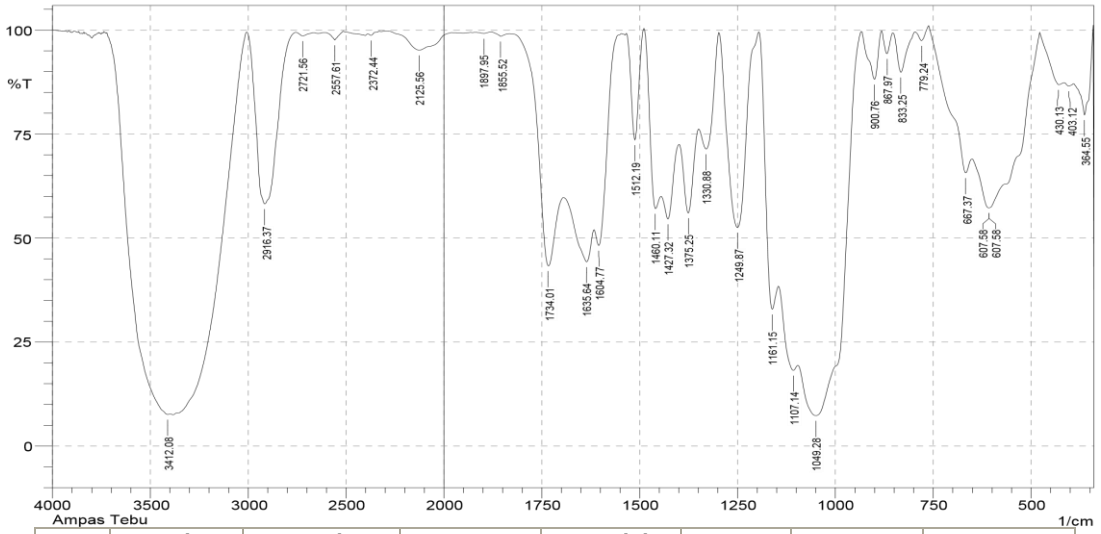

No.	Peak	Intensity	Corr. Intensity	Base (H)	Base (L)	Area	Corr. Area
1	364.55	79.611	13.715	391.55	343.33	3.372	1.789
2	403.12	86.577	0.648	414.7	393.48	1.3	0.041
3	430.13	86.885	3.415	478.35	414.7	2.529	0.583
4	607.58	57.291	19.213	650.01	478.35	27.825	13.915
5	607.58	57.291	19.49	651.94	478.35	28.289	14.085
6	667.37	65.66	7.853	761.88	651.94	10.367	1.606
7	779.24	97.495	2.833	796.6	761.88	0.165	0.214
8	833.25	89.902	9.53	852.54	796.6	1.239	1.112
9	867.97	94.338	5.237	881.47	852.54	0.405	0.35
10	900.76	88.187	11.49	931.62	883.4	1.454	1.382
11	1049.28	7.301	35.047	1095.57	933.55	108.693	52.091
12	1107.14	18.169	5	1145.72	1097.5	30.302	2.871
13	1161.15	32.873	23.178	1193.94	1147.65	14.085	4.097
14	1249.87	52.541	46.854	1296.16	1195.87	13.323	13.065
15	1330.88	71.41	12.813	1348.24	1298.09	5.084	2.17
16	1375.25	56.054	18.218	1398.39	1350.17	9.057	2.863
17	1427.32	54.58	10.349	1444.68	1400.32	9.411	1.488
18	1460.11	57.079	15.774	1489.05	1446.61	6.659	1.851
19	1512.19	73.593	26.067	1533.41	1490.97	2.688	2.628
20	1604.77	48.206	11.681	1616.35	1546.91	9.846	1.64
21	1635.64	44.282	9.41	1693.5	1618.28	22.208	3.024
22	1734.01	43.316	27.667	1830.45	1695.43	20.237	6.834
23	1855.52	98.506	0.841	1876.74	1832.38	0.197	0.069
24	1897.95	99.19	0.339	1923.03	1882.52	0.11	0.025
25	2125.56	95.188	4.367	2279.86	1980.89	3.516	2.942
26	2372.44	98.737	0.529	2387.87	2331.94	0.193	0.048
27	2557.61	97.627	1.99	2611.62	2515.18	0.508	0.339
28	2721.56	98.602	0.838	2758.21	2667.55	0.378	0.154
29	2916.37	58.216	41.294	3007.02	2758.21	26.349	25.809
30	3412.08	7.598	3.888	3722.61	3398.57	184.913	12.916

Comment; Ampas Tebu

Date/Time; 12/16/2020 1:35:11 PM

No. of Scans;

- Hasil FTIR Selulosa Ampas Tebu

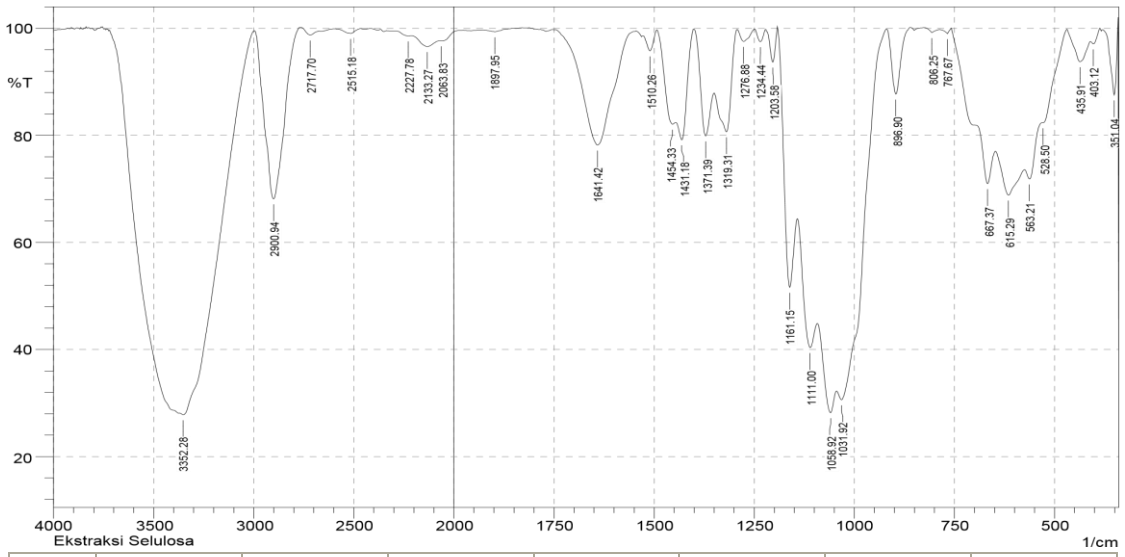

No.	Peak	Intensity	Corr. Intensity	Base (H)	Base (L)	Area	Corr. Area
1	351.04	87.525	13.942	379.98	341.4	0.917	1.065
2	403.12	97.066	1.293	410.84	387.69	0.205	0.08
3	435.91	93.754	4.776	468.7	410.84	1.023	0.679
4	528.5	82.35	0.571	530.42	470.63	2.475	0.102
5	563.21	71.835	4.15	574.79	532.35	4.986	0.451
6	615.29	68.814	6.618	646.15	576.72	10.025	1.42
7	667.37	70.955	7.959	698.23	648.08	5.917	0.897
8	767.67	98.972	0.968	786.96	758.02	0.061	0.048
9	806.25	99.169	0.776	825.53	786.96	0.056	0.046
10	896.9	87.688	12.253	918.12	862.18	1.335	1.331
11	1031.92	30.586	7.981	1043.49	920.05	30.955	3.736
12	1058.92	28.192	7.704	1091.71	1045.42	21.979	2.407
13	1111	40.371	11.521	1141.86	1093.64	15.884	2.736
14	1161.15	51.587	25.922	1190.08	1143.79	8.443	3.775
15	1203.58	93.658	6.423	1220.94	1192.01	0.407	0.411
16	1234.44	97.504	2.322	1249.87	1220.94	0.175	0.154
17	1276.88	97.54	2.268	1292.31	1249.87	0.268	0.235
18	1319.31	80.646	13.752	1350.17	1294.24	3.525	1.973
19	1371.39	79.892	12.704	1400.32	1352.1	2.884	1.453
20	1431.18	79.168	8.766	1444.68	1402.25	2.618	0.903
21	1454.33	82.077	3.199	1492.9	1446.61	2.478	0.461
22	1510.26	95.778	3.382	1527.62	1492.9	0.389	0.261
23	1641.42	78.157	21.413	1745.58	1550.77	8.777	8.42
24	1897.95	99.321	0.509	1928.82	1853.59	0.116	0.071
25	2063.83	97.631	0.262	2075.41	1984.75	0.633	0.085
26	2133.27	96.569	1.488	2210.42	2075.41	1.562	0.448
27	2227.78	98.565	0.208	2297.22	2212.35	0.38	0.031
28	2515.18	99.027	0.883	2582.68	2468.88	0.264	0.216
29	2717.7	98.736	1.069	2767.85	2673.34	0.28	0.208
30	2900.94	68.14	31.671	2995.45	2771.71	16.82	16.686
31	3352.28	27.792	3.659	3369.64	2997.38	97.933	4.592

Comment Date/Time; 12/16/2020 1:29:51 PM
Ekstraksi Selulosa No. of Scans;

- Hasil FTIR Aerogel Selulosa

SHIMADZU

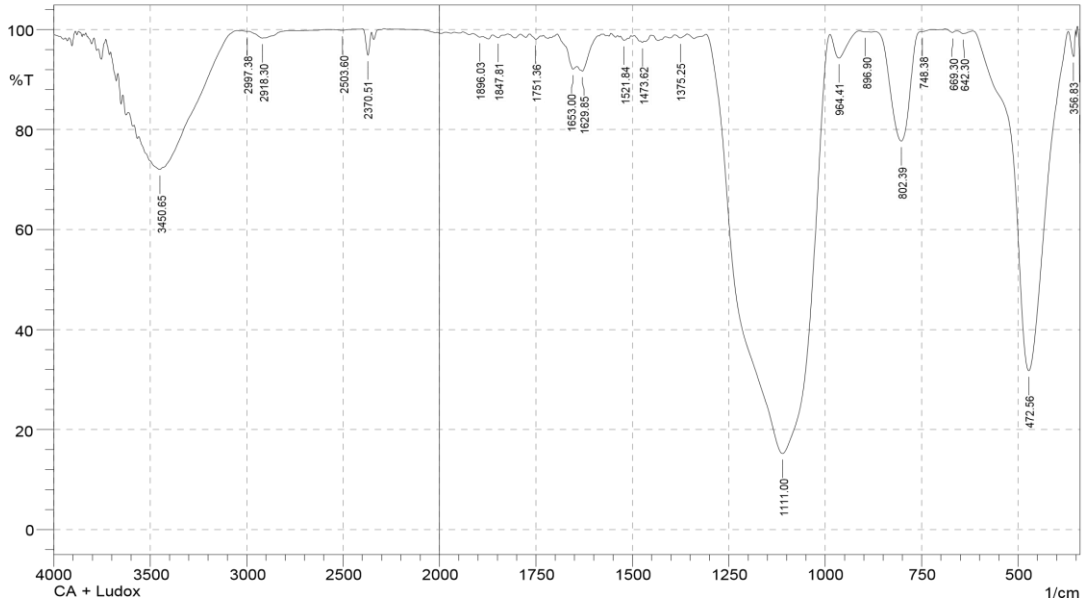

No.	Peak	Intensity	Corr. Intensity	Base (H)	Base (L)	Area	Corr. Area
1	356.83	94.597	5.155	370.33	351.04	0.246	0.222
2	472.56	31.738	67.918	615.29	370.33	38.204	37.843
3	642.3	99.175	0.544	657.73	617.22	0.096	0.046
4	669.3	99.407	0.468	688.59	657.73	0.037	0.027
5	748.38	99.574	0.066	752.24	725.23	0.027	0.002
6	802.39	77.689	21.896	869.9	754.17	5.816	5.608
7	896.9	99.52	0.08	912.33	891.11	0.037	0.004
8	964.41	94.273	4.968	987.55	912.33	0.984	0.782
9	1111	15.176	83.798	1307.74	989.48	129.729	128.317
10	1375.25	98.302	0.721	1390.68	1357.89	0.191	0.052
11	1473.62	97.438	0.262	1479.4	1469.76	0.104	0.006
12	1521.84	97.845	0.627	1531.48	1512.19	0.158	0.029
13	1629.85	91.685	2.472	1643.35	1589.34	1.249	0.242
14	1653	92.059	1.604	1693.5	1645.28	1.02	0.11
15	1751.36	98.052	0.859	1766.8	1737.86	0.191	0.055
16	1847.81	98.367	0.621	1861.31	1822.73	0.212	0.046
17	1896.03	98.455	0.338	1913.39	1888.31	0.135	0.016
18	2370.51	94.88	4.832	2399.45	2353.16	0.472	0.431
19	2503.6	99.831	0.221	2567.25	2420.66	0.014	0.051
20	2918.3	98.292	1.401	2989.66	2763.99	0.881	0.603
21	2997.38	99.623	0.058	3026.31	2989.66	0.051	0.007
22	3450.65	71.998	11.106	3558.67	3051.39	40.581	14.165

Comment;

CA + Ludox

Date/Time; 3/5/2021 3:42:21 PM No. of Scans;

- Hasil FTIR Aerogel Selulosa Modifikasi CTAB

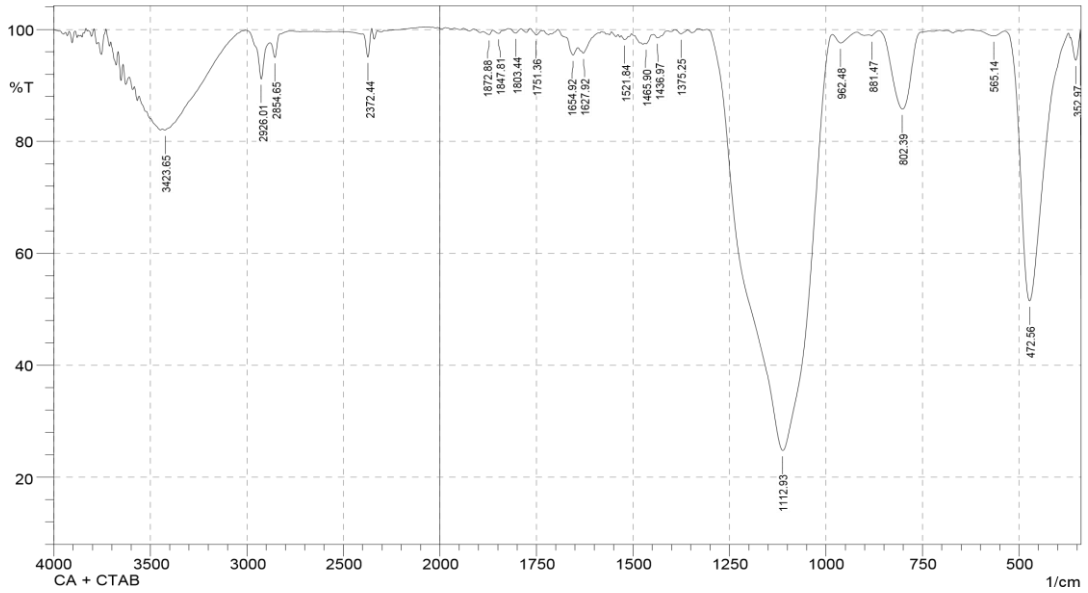

No.	Peak	Intensity	Corr. Intensity	Base (H)	Base (L)	Area	Corr. Area
1	352.97	94.509	4.755	366.48	341.4	0.389	0.303
2	472.56	51.477	48.051	536.21	374.19	17.45	17.078
3	565.14	98.863	0.892	609.51	536.21	0.218	0.143
4	802.39	85.782	13.965	862.18	734.88	3.52	3.379
5	881.47	98.85	0.417	891.11	862.18	0.091	0.015
6	962.48	97.596	1.645	983.7	920.05	0.412	0.221
7	1112.93	24.779	74.694	1307.74	983.7	88.364	87.747
8	1375.25	99.218	0.741	1392.61	1357.89	0.06	0.053
9	1436.97	98.496	0.771	1446.61	1408.04	0.159	0.063
10	1465.9	97.429	0.387	1469.76	1446.61	0.177	0.007
11	1521.84	98.178	0.656	1529.55	1512.19	0.119	0.03
12	1627.92	95.761	1.763	1643.35	1589.34	0.6	0.145
13	1654.92	95.409	2.098	1672.28	1643.35	0.433	0.139
14	1751.36	99.015	0.964	1766.8	1737.86	0.062	0.061
15	1803.44	99.355	0.817	1822.73	1789.94	0.031	0.056
16	1847.81	99.276	0.71	1863.24	1822.73	0.051	0.056
17	1872.88	99.088	0.677	1888.31	1863.24	0.066	0.037
18	2372.44	95.067	4.683	2397.52	2353.16	0.478	0.418
19	2854.65	94.987	3.391	2881.65	2825.72	0.714	0.322
20	2926.01	91.172	7.248	3005.1	2881.65	1.885	1.197
21	3423.65	82.022	0.819	3439.08	3007.02	17.907	0.689

Comment;

CA + CTAB

Date/Time; 3/5/2021 3:48:16 PM

No. of Scans;

- Zat warna *Methyl Orange*

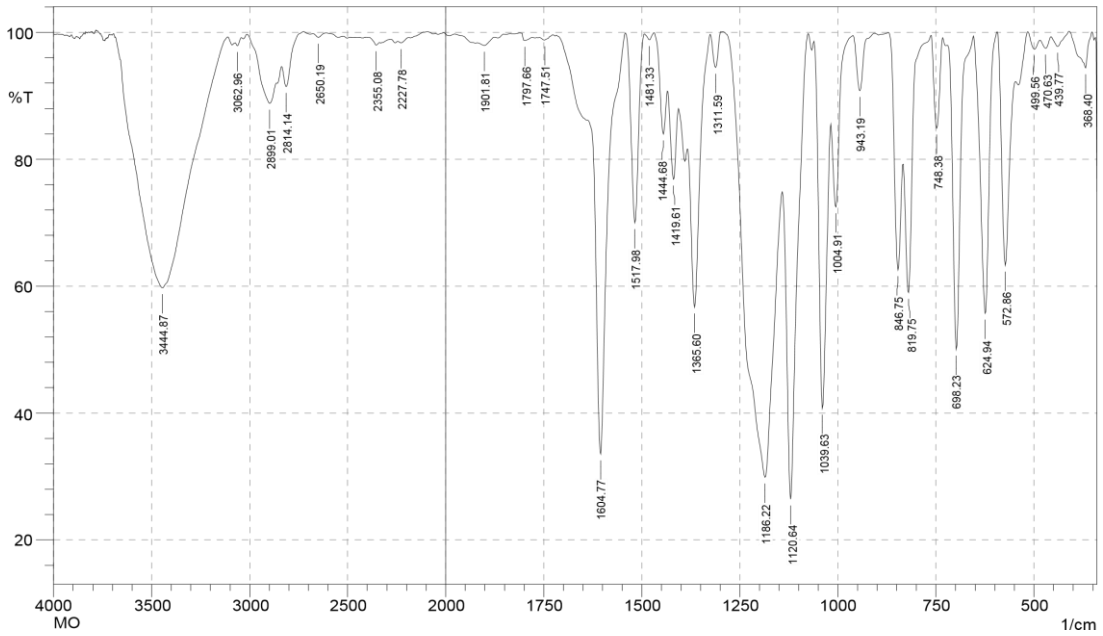

No.	Peak	Intensity	Corr. Intensity	Base (H)	Base (L)	Area	Corr. Area
1	368.4	94.408	5.672	410.84	352.97	0.699	0.726
2	439.77	97.78	1.849	457.13	410.84	0.243	0.19
3	470.63	97.499	1.536	484.13	457.13	0.216	0.102
4	499.56	97.349	2.043	516.92	484.13	0.232	0.15
5	572.86	63.278	33.226	592.15	547.78	4.46	3.628
6	624.94	55.715	44.031	653.87	594.08	5.728	5.667
7	698.23	50.03	48.309	719.45	655.8	5.836	5.434
8	748.38	84.899	14.221	761.88	734.88	1.134	1.028
9	819.75	59.003	24.18	833.25	763.81	4.62	2.032
10	846.75	62.564	23.533	869.9	835.18	3.884	2.057
11	943.19	90.808	8.827	962.48	906.54	0.805	0.729
12	1004.91	72.486	16.41	1018.41	962.48	2.778	1.2
13	1039.63	40.737	50.526	1060.85	1020.34	7.945	6.285
14	1120.64	26.409	56.54	1141.86	1076.28	14.866	10.847
15	1186.22	29.877	51.977	1292.31	1143.79	37.92	28.447
16	1311.59	94.458	5.455	1325.1	1298.09	0.349	0.339
17	1365.6	56.685	30.502	1382.96	1327.03	6.231	3.794
18	1419.61	76.851	12.448	1433.11	1406.11	2.255	0.914
19	1444.68	83.955	9.479	1467.83	1435.04	1.359	0.628
20	1481.33	98.836	1.012	1492.9	1469.76	0.068	0.053
21	1517.98	69.974	29.839	1541.12	1494.83	3.035	2.996
22	1604.77	33.539	57.352	1637.56	1543.05	13.653	10.615
23	1747.51	98.783	0.586	1761.01	1728.22	0.13	0.045
24	1797.66	98.74	0.9	1809.23	1778.37	0.122	0.061
25	1901.81	97.954	0.76	1919.17	1876.74	0.297	0.073
26	2227.78	98.35	0.409	2243.21	2189.21	0.309	0.046
27	2355.08	97.996	0.65	2393.66	2337.72	0.349	0.057

Date/Time; 7/23/2021 11:20:49 AM No. of Scans;

Resolution;

- Hasil FTIR AS Modifikasi CTAB setelah adsorpsi *Methyl Orange*

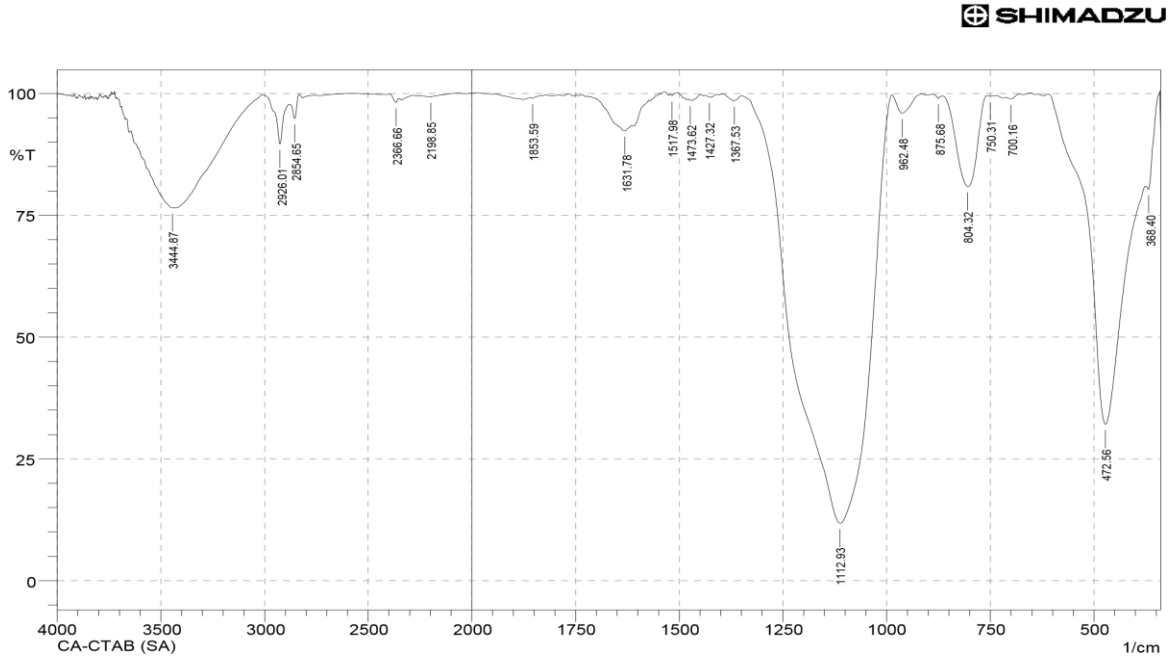

No.	Peak	Intensity	Corr. Intensity	Base (H)	Base (L)	Area	Corr. Area
1	368.4	80.356	3.02	372.26	343.33	1.308	0.136
2	472.56	32.129	56.543	609.51	378.05	41.758	30.98
3	700.16	98.906	0.563	711.73	682.8	0.1	0.042
4	750.31	99.454	0.121	758.02	734.88	0.049	0.007
5	804.32	80.875	18.634	864.11	759.95	4.944	4.719
6	875.68	99.001	0.623	891.11	866.04	0.058	0.021
7	962.48	95.955	3.82	987.55	916.19	0.658	0.596
8	1112.93	11.775	87.817	1350.17	989.48	136.209	135.544
9	1367.53	98.56	1.106	1396.46	1350.17	0.174	0.116
10	1427.32	99.259	0.072	1438.9	1425.4	0.033	0.001
11	1473.62	98.623	0.125	1479.4	1471.69	0.043	0.003
12	1517.98	99.524	0.416	1521.84	1510.26	0.01	0.009
13	1631.78	92.37	1.151	1651.07	1616.35	1.115	0.106
14	1853.59	98.983	0.29	1859.38	1843.95	0.056	0.009
15	2198.85	99.331	0.483	2283.72	2079.26	0.327	0.195
16	2366.66	98.181	1.08	2395.59	2353.16	0.199	0.091
17	2854.65	94.847	4.039	2879.72	2833.43	0.595	0.351
18	2926.01	89.629	8.834	3008.95	2879.72	2.182	1.467
19	3444.87	76.525	0.597	3608.81	3437.15	15.496	1.072

Comment; Date/Time; 7/23/2021 11:14:54

CA-CTAB (SA) AM No. of Scans;

Resolution; Apodization;

Lampiran 4. Hasil karakterisasi dengan SEM

KEMENTERIAN RISET TEKNOLOGI DAN PENDIDIKAN TINGGI
UNIVERSITAS DIPONEGORO
UPT LABORATORIUM TERPADU
Jalan Prof. Soedarto, SH Tembalang Semarang Kotak Pos 1269
Telepon (024) 76918147- Faksimile (024) 76918148, Website :
http://labterpadu.undip.ac.id;
E-mail : labterpadu@live.undip.ac.id

Hasil Uji Citra SEM sbb:

Aerogel Selulosa

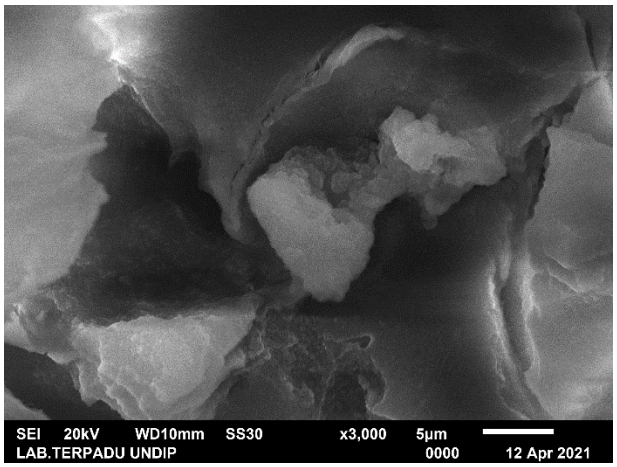

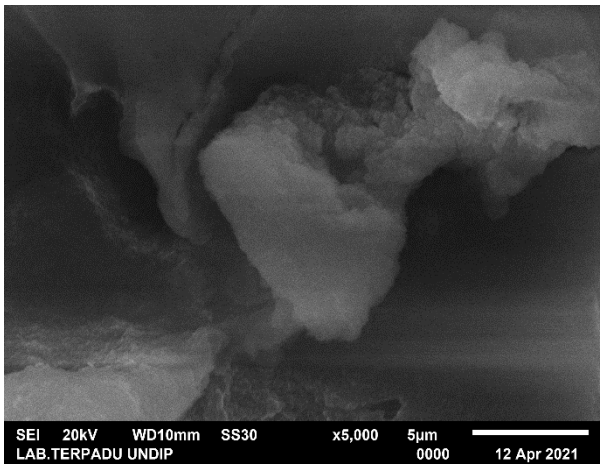

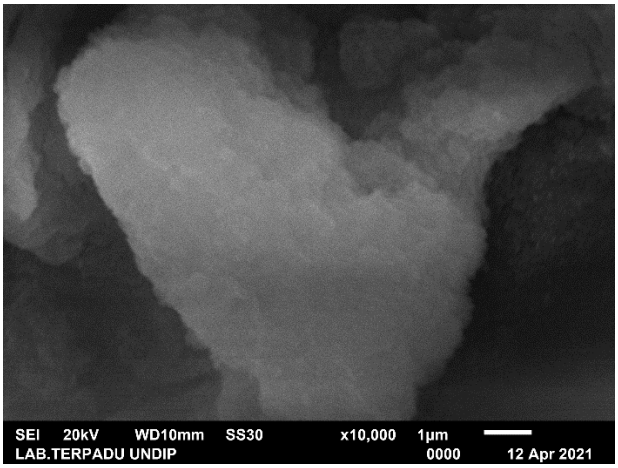

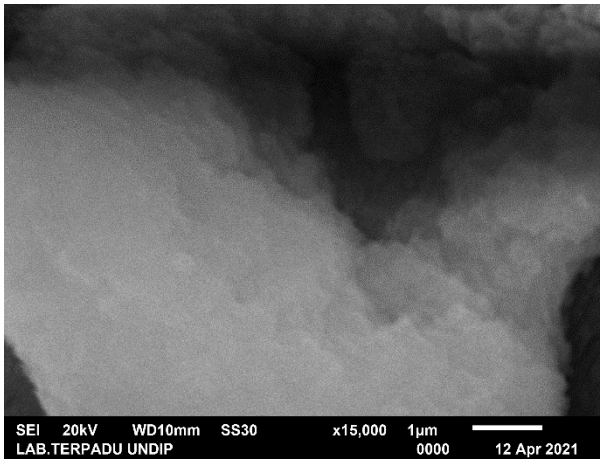

KEMENTERIAN RISET TEKNOLOGI DAN PENDIDIKAN TINGGI
UNIVERSITAS DIPONEGORO
UPT LABORATORIUM TERPADU
Jalan Prof. Soedarto, SH Tembalang Semarang Kotak Pos 1269
Telepon (024) 76918147- Faksimile (024) 76918148, Website :
http://labterpadu.undip.ac.id;
E-mail : labterpadu@live.undip.ac.id

Hasil Uji Citra SEM sbb:

Aerogel Selulosa Modifikasi CTAB

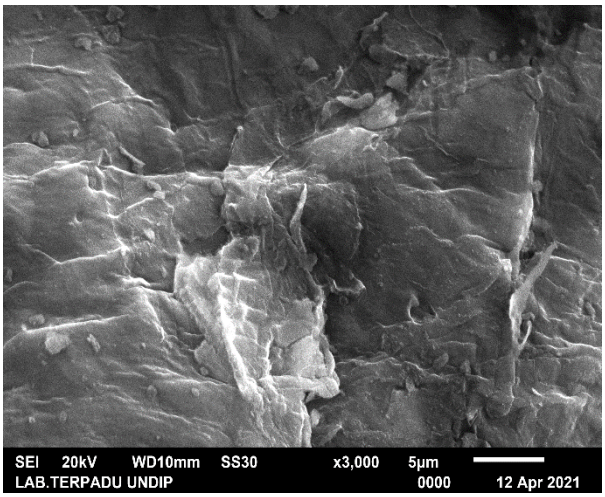

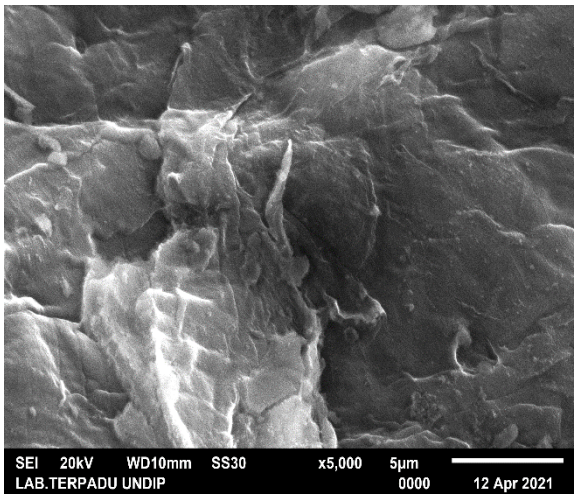

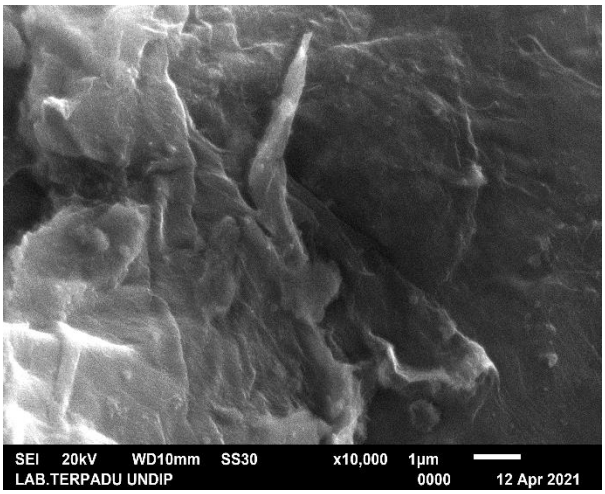

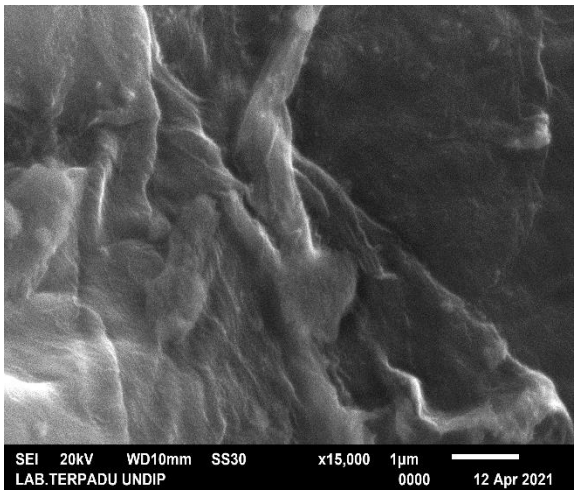

KEMENTERIAN RISET TEKNOLOGI DAN PENDIDIKAN TINGGI
UNIVERSITAS DIPONEGORO
UPT LABORATORIUM TERPADU
Jalan Prof. Soedarto, SH Tembalang Semarang Kotak Pos 1269
Telepon (024) 76918147- Faksimile (024) 76918148, Website :
http://labterpadu.undip.ac.id;
E-mail : labterpadu@live.undip.ac.id

Hasil Uji Citra SEM sbb:

Aerogel Selulosa Modifikasi CTAB setelah Adsorpsi *Methyl Orange*

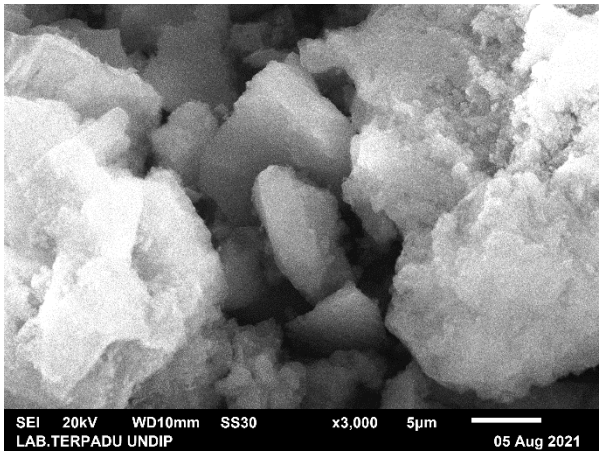

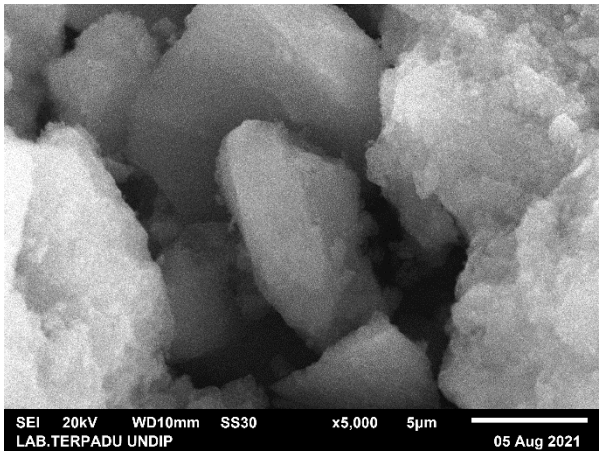

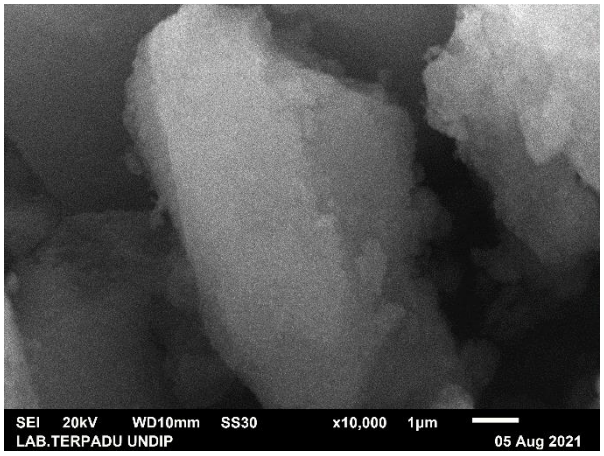

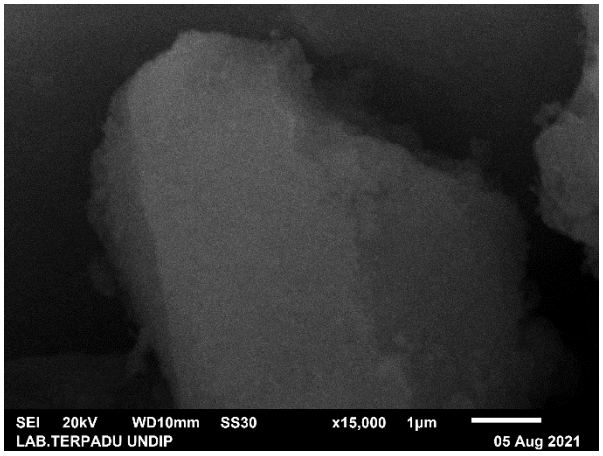

Lampiran 5. Karakterisasi Luas Permukaan dengan Metode Metilen Biru

1. Penentuan λmax. metilen biru

Panjang Gelombang	Absorbansi
630	0,478
635	0,497
640	0,531
645	0,556
650	0,576
655	0,59
656	0,59
657	0,591
658	0,591
659	0,591
660	0,595
661	0,595
662	0,596
663	0,596
664	0,606
665	0,59
670	0,514
675	0,456
680	0,387
685	0,317
690	0,241

Kurva hubungan antara absorbansi dan panjang gelombang *methyl orange*:

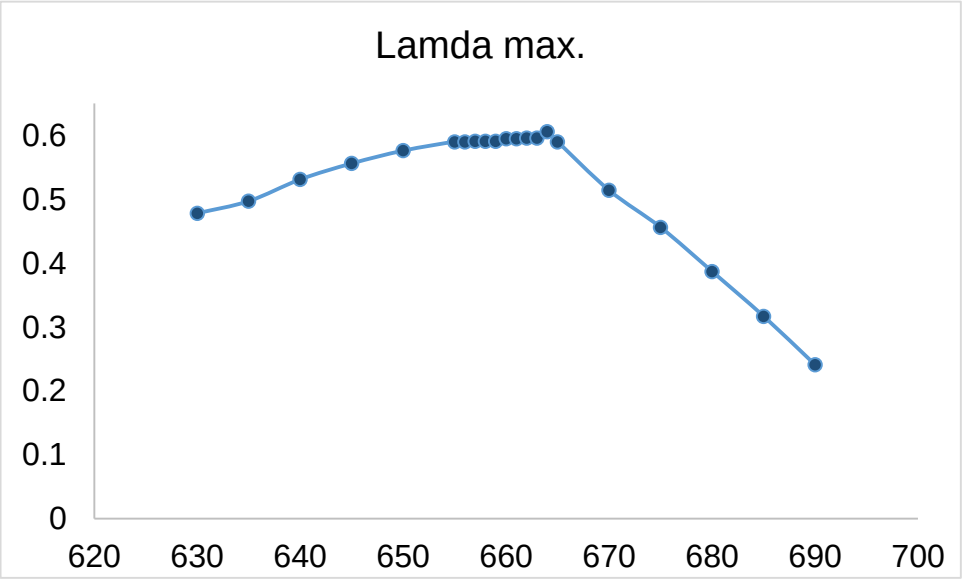

2. Penentuan Absorbansi Deret Standar Metilen Biru

Konsentrasi (mg/L)	Absorbansi
1	0,097
2	0,188
4	0,378
8	0,71
10	0,894

Kurva standar *methyl orange* dengan spektrofotometer UV-Vis:

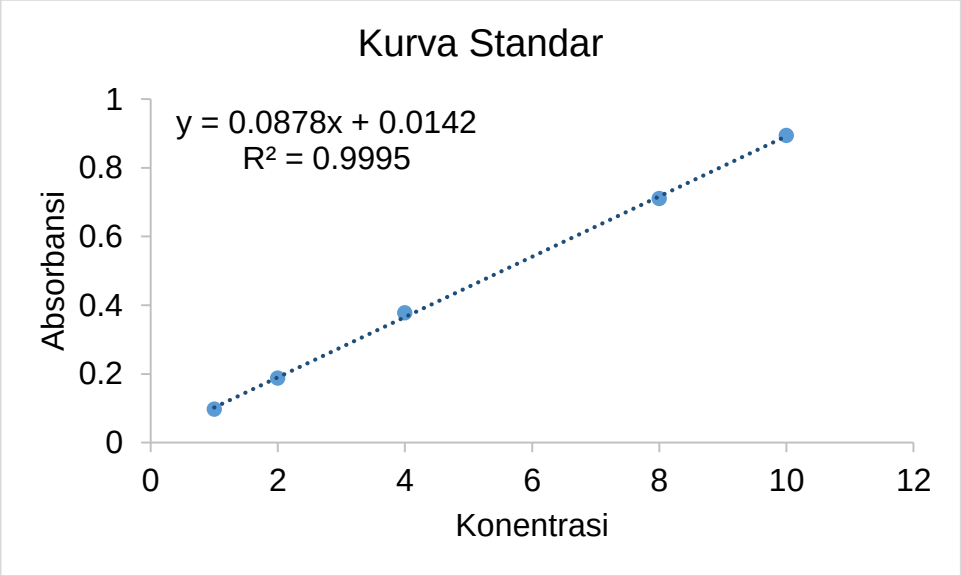

3. Penentuan Luas Permukaan

Data penentuan luas permukaan dengan larutan metiln biru menggunakan volume 50 mL:

Abs.	FP	Co (mg/L)	Ce (mg/L)	Wa (g)	qe (mg/g)	S (m^2/g)
1,194	100	2869,97	1359,74	0,3037	248,642	920
1,328	100	2869,97	1512,37	0,3042	223,148	826

$$q_e = \frac{(C_o - C_e)V}{W}$$

Contoh perhitungan jumlah metilen biru yang diadsorpsi (q_e):

$$q_e = \frac{(2869{,}97\text{-}1359{,}74\ )\frac{mg}{L}}{0.3037} \times 0{,}05\ L$$

$$q_e = 248{,}642\ mg/g$$

Contoh perhitunan luas permukaan adsorben (S):

$$S = \frac{X_m\ .\ V\ .\ a}{Mr}$$

$$S = \frac{(2869{,}97\ x\ \ 6{,}02\ x\ \ 197)}{320{,}5\ g/mol}$$

$$S = 920$$

Lampiran 6. Data Penentuan Panjang Gelombang Maksimum *Methyl orange*

Hubungan antara absorbansi dan panjang gelombang *methyl orange* konsentrasi 2 mg/L:

Panjang gelombang (nm)	Absorbansi
435	0,442
440	0,468
445	0,48
450	0,49
455	0,494
460	0,498
465	0,492
470	0,482
475	0,46
480	0,438

Kurva hubungan antara absorbansi dan panjang gelombang *methyl orange* dengan konsentrasi 2 mg/L:

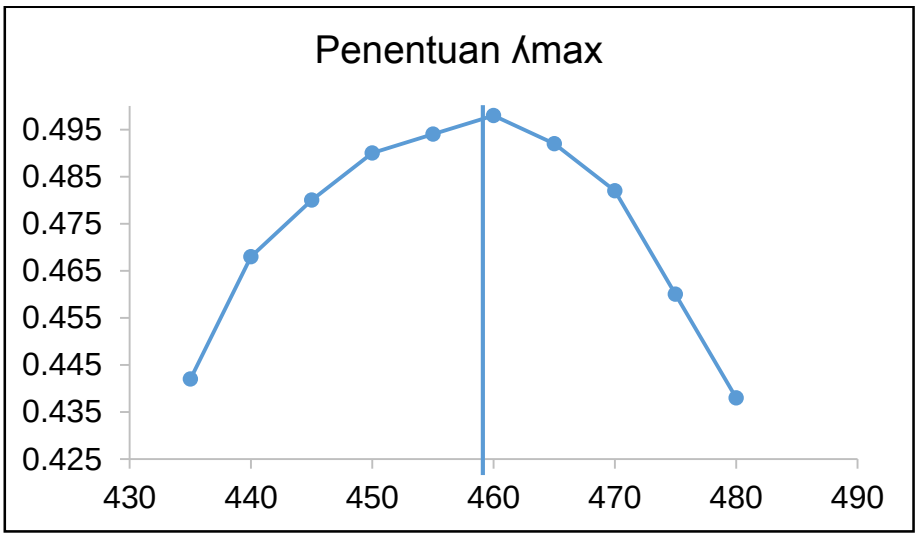

Lampiran 7. Penentuan Absorbansi Deret Standar Larutan *Methyl orange*

Hubungan antara absorbansi dan konsentrasi *methyl orange*:

Konsentrasi	Absorbansi
2	0,173
4	0,302
6	0,444
8	0,59
10	0,732

Kurva standar *methyl orange* dengan spektrofotometer UV-Vis:

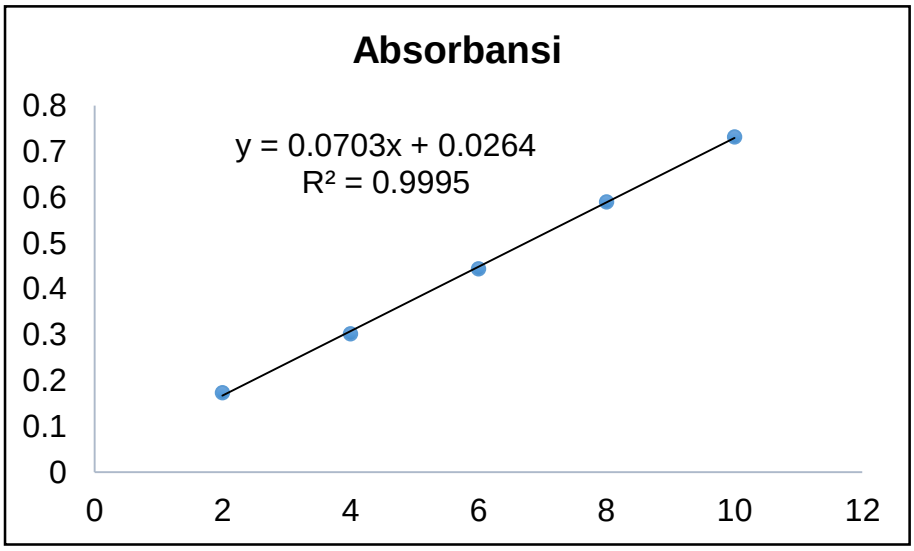

Lampiran 8. Penentuan Waktu Optimum

Data penentuan waktu optimum adsorpsi *methyl orange* oleh aerogel selulosa:

Waktu Kontak (menit)	Abs.	FP	Ce (mg/L)	Co (mg/L)	W (g)	q_e (mg/g)
60	1.35	5	95,6415	100	0,1017	0,3867
120	1,35	5	95,6415	100	0,1025	0,3875
180	1,35	5	95,6415	100	0,1003	0,3875
240	1,35	5	95,6415	100	0,1003	0,3875
300	1,34	5	94,9303	100	0,1018	0,7357

$$q_e = \frac{(C_o - C_e)V}{W}$$

Contoh perhitungan jumlah *methyl orange* yang diadsorpsi (q_e) pada t = 5 jam

$$q_e = \frac{(100\text{-}94{,}9303)\,\frac{mg}{L}}{0{,}1018} \times 0{,}05\ L$$

$$q_e = 0{,}7357\ mg/g$$

Data penentuan waktu optimum adsorpsi *methyl orange* oleh aerogel selulosa termodifikasi CTAB:

Waktu Kontak	Absorbansi	Ce (mg/L)	Co (mg/L)	W (g)	q_e (mg/g)
5	1,95	27,36273	100	0,1016	34,65181
10	1,8	25,22902	100	0,1021	35,52702
20	1,74	24,37553	100	0,1006	36,48095
30	1,7	23,80654	100	0,1007	36,72724
45	1,64	22,95306	100	0,1006	37,18794
60	1,62	22,66856	100	0,1005	37,36649
75	**1,5**	**20,96159**	**100**	**0,1009**	**38,10199**
90	1,46	20,39260	100	0,1022	37,8584

$$q_e = \frac{(C_o - C_e)V}{W}$$

Contoh perhitungan jumlah *methyl orange* yang diadsorpsi (q_e) pada t = 75 menit

$$q_e = \frac{(100\text{-}20{,}96159\ )\frac{mg}{L}}{0{,}1008} \times 0{,}05\ L$$

$$q_e = 38{,}10199\ mg/g$$

Lampiran 9. Data Kinetika Adsorpsi

Persamaan kinetika *pseudo*-orde 1 yaitu:

$$\ln(q_t\text{-}q_e) = \ln qe\text{-}kt$$

Waktu	qe	qt	ln (qe-qt)	t/q
5	34,65181	38,10199	1,2384	0,1443
10	35,52702	38,10199	0,9458	0,2815
20	36,48095	38,10199	0,4831	0,5482
30	36,72724	38,10199	0,3183	0,8168
45	37,18794	38,10199	-0,0899	1,2101
60	37,36649	38,10199	-0,3072	1,6057
75	38,10199	38,10199	0	1,9684
90	37,85841	38,10199	-1,4123	2,3773

Dari grafik kinetika orde pertama semu diperoleh persamaan garis:

y = -0,0243x + 1,1648

dari persamaan garis diperoleh nilai *slope* (a) = -0,0243x dan *intercept* (b) = 1,1648

nilai k_1 dapat dihitung sebagai berikut:

k_1 = -0,0243 menit^{-1}

ln q_e = intercept

q_e = 1,1648= 3,2053 (mg/g)

R^2 = 0,8503

- Persamaan kinetika orde kedua semu yaitu:

$$\frac{t}{q_e} = \frac{1}{k_2 q_e^2} + \frac{1}{q_t} 1$$

Dari grafik kinetika orde kedua semu diperoleh persamaan garis:

y = 0,0262x + 0,0235

dari persamaan garis diperoleh nilai *slope* (a) = 0,0262x dan *intercept* (b) = 0,0235

nilai k_2 dapat dihitung sebagai berikut:

$$slope = \frac{1}{q_e} \qquad q_e = \frac{1}{0{,}027} = 38{,}1679 \text{ (mg/g)}$$

$$intercept = \frac{1}{k_2 q_e^2} \qquad k_2 = \frac{1}{0{,}0235 \times (38{,}1679)^2} = 0{,}0292 \text{ g/mg min}^{-1}$$

k_2 = 0,0292 g/mg min^{-1}

R^2 = 0,9998

Lampiran 10. Penentuan Suhu Optimum

Data penentuan suhu optimum adsorpsi *methyl orange* oleh aerogel selulosa termodifikasi CTAB:

Suhu	Absorbansi	Ce (mg/L)	Co (mg/L)	W (g)	q_e (mg/g)
40	1,52	21,2461	100	0,1008	37,2553
50	1,37	19,1124	100	0,1008	38,6665
60	1,32	18,4011	100	0,1010	39,2941

$$q_e = \frac{(C_o - C_e)V}{W}$$

Contoh perhitungan jumlah *methyl orange* yang diadsorpsi (q_e) pada Suhu 30 °C.

$$q_e = \frac{(100\text{-}21{,}2461)\frac{\text{mg}}{\text{L}}}{0.1010} \times 0.05 \text{ L}$$

$$q_e = 37{,}1815 \text{ mg/g}$$

Lampiran 11. Data Termodinamika

Parameter termodinamika dari proses adsorpsi ditentukan dari data eksperimen yang diperoleh diberbagai suhu menggunakan persamaan berikut:

$$K_c = \frac{q_e}{C_e}$$

$$\Delta G° = -R\,T\,\ln Kc$$

$$\ln K_c = \frac{\Delta S°}{R} - \frac{\Delta H°}{RT}$$

Berdasarkan persamaan di atas, diperoleh data termodinamika adsorpsi *methyl orange* oleh aerogel selulosa termodifikasi CTAB sebagai berikut:

T (K)	1/T	qe/ce	ln Kc	ΔG°	ΔH° (kJ/mol)	ΔS° (J/mol.K)
313	0,003195	1,7535	0,5616	-1,4615	+25,2022	+32,1752
323	0,003096	2,0231	0,7046	-1,8923		
333	0,003003	2,1354	0,7587	-2,1004		

Dari grafik antara 1/T terhadap ln Kc, diperoleh persamaan dengan nilai *slope* (a) = -3031,3 dan *intercept* (b) = 3,87

Nilai k_1 = -3031,3 Nilai K = 3,87

$\frac{\Delta H}{R}$ = -*slope* $\frac{\Delta S}{R}$ = *intercept*

$\frac{\Delta H}{R}$ = -(-3031,3) $\frac{\Delta S}{R}$ = 3,87

ΔH= +25,2022 kJ/mol ΔS= +32,1752 J/mol.K

Lampiran 12. Penentuan Kapasitas Adsorpsi

$$q_e = \frac{(C_o - C_e)V}{W}$$

Co (mg/L)	Abs.	FP	Ce (mg/L	W (g)	qe (mg/g)	Ce/qe	Log Ce	Log qe
119,4679	1,8	-	25,22901	0,1004	46,93176	0,5376	1,4019	1,67146
153,2517	0,165	25	58,30156	0,1004	47,28596	1,2329	1,7657	1,67473
185,9687	0,237	25	83,90611	0,1004	50,82798	1,6508	1,9238	1,70610
242,1564	0,384	25	136,1820	0,1007	52,61887	2,5881	2,1341	1,72114
272,0284	0,466	25	165,3428	0,1007	52,97201	3,1213	2,2184	1,72404
307,2347	0,562	25	199,4822	0,1008	53,44866	3,7322	2,2999	1,72793

Contoh perhitungan jumlah *methyl orange* yang diadsorpsi (q_e) pada konsentrasi 307.2347:

$$q_e = \frac{(307{,}2347\text{-}199{,}4822)\,\frac{mg}{L}}{0{,}1008} \times 0{,}05\ L$$

$$q_e = 199{,}4822$$

- Isotermal Langmuir

$$\frac{C_e}{q_e} = \frac{1}{Q_o b} + \frac{C_e}{Q_o}$$

Berdasarkan model isotermal Langmuir diperoleh persamaan garis:

$$y = 0{,}0181x + 0{,}1241$$

dari persamaan garis tersebut, nilai *slope* = 0,0181 dan *intercept* = 1,202

- Perhitungan nilai Qo

$$\frac{1}{Q_o} = \text{kimiringan } (slope)$$

$$Q_o = \frac{1}{slope}$$

$$Q_o = 55{,}24862 \text{ mg/g}$$

- Perhitungan nilai b

$$\frac{1}{\mathrm{Q_o b}} = \mathrm{intercept}$$

$$\mathrm{b} = \frac{1}{\mathrm{Q_o} \times \mathrm{intercept}}$$

= 0,14585 L/mg

- Isotermal Freundlich

$$\log Q_e = \log k \ + \ {}^{1}/_{n} \ \log \ (C_e)$$

Berdasarkan model isotermal Freundlich diperoleh persamaan garis:

$$y = 0{,}0712x \ + \ 1{,}565$$

dari persamaan garis tersebut, nilai *slope* = 0,0712 dan *intercept* = 1,565

log k = *intercept*

- Perhitungan nilai k

k = *invers* log *intercept*

= *invers* log 1,565

= 36,7282 mg/g

- Perhitungan nilai n

$$\frac{1}{\mathrm{n}} = slope$$

$$\mathrm{n} = \frac{1}{slope}$$

$$\mathrm{n} = \frac{1}{0{,}0712 \ \mathrm{L/g}}$$

$$\mathrm{n} = 14{,}0449 \ \mathrm{g/L}$$

Lampiran 13. Persen Efektivitas Adsorpsi Limbah Zat Warna oleh Aerogel Selulosa Termodifikasi CTAB

Data limbah zat warna (*titan yellow, methyl orange* dan *congo red*) diukur pada panjang gelombang maksimum masing-masing zat warna yaitu 400 nm, 496 nm dan 460 nm.

Zat warna	Abs.	a	b	Co (mg/L)	Ce (mg/L)	% Efeltivitas
Titan Yellow	0,273	0,0547	0,048	66,76	4,11	93,84
Methyl Orange	0,382	0,0703	0,0264	51,12	5,06	90,10
Congo Red	0,240	0,0328	0,0674	60,89	9,37	84,61

$$q\% = \frac{C_{awal}-C_{akhir}}{C_{awal}} x100$$

Contoh perhitungan % kapasitas adsorpsi limbah zat warna *methyl orange* yang diadsorpsi dengan perbandingan 1:1:1 untuk masing-masing zat warna.

$$q\% = \frac{51,12 - 4,11}{51,12} x100$$

$$= 90,10\%$$